FINAL REPORT

ON

GLOBAL THUNDERSTORM ACTIVITY RESEARCH SURVEY

Contract No. NAS-8-34587

Prepared by

Samuel C. Coroniti
Samuel C. Coroniti, Inc.
3305 Mill Springs Drive
Fairfax, Virginia 22031

Prepared for

Atmospheric Sciences Division,
Space Science Laboratory
George C. Marshall Space Flight Center
Marshall Space Flight Center, ALA 35812

May 15, 1982

ACKNOWLEDGMENTS

The author is indebted to Dr. James C. Dodge, Manager of Severe Storms and Local Weather Research, NASA Headquarters, Washington, D. C., for his support of this research. Special thanks to Otha H. Vaughn, Jr. of the Marshall Space Flight Center, who was the scientific monitor of this research. The author is indebted for the use of the Technical Library at the NASA Goddard Space Flight Center, Greenbelt, MD.

ABSTRACT

The published literature on the subject of the monitoring of global thunderstorm activity by instrumented satellites has been reviewed. A survey of the properties of selected physical parameters of the thunderstorm is presented. The concepts used by satellites to identify and to measure terrestrial lightning pulses are described. Included also is a discussion on the experimental data acquired by satellites. The scientific achievements of the satellites are evaluated against the needs of scientists and the potential requirements of user agencies. The performances of the satellites are rated according to their scientific and operational achievements. Finally, recommendations for additional studies and experiments are made.

TABLE OF CONTENTS

I - Introduction

By observing the percentage of days per year on which thunder was heard in each region of the earth, Brooks (1) developed global maps of seasonal and annual frequency of thunderstorms. He estimated, in 1925, the number of global thunderstorms per annum to be approximately 16×10^6, on average the number of storms occurring in any given time to be 1800, and the number of lightning strokes occurring per second to be approximately 100. From 1925 to the present time, many electrical ground-based systems were developed and used to determine more precisely the number of global thunderstorms. They, however, lack the capability of counting precisely the number of thunderstorms over the oceans. In the early 1960s, electrical and optical pulses produced by terrestrial lightning were detected and recorded by instruments on orbiting satellites. These early experimental results indicated that a satellite could be a suitable platform from which global thunderstorm activity could be monitored more precisely.

The satellites, as reported in the open scientific literature, that detected global terrestrial lightning flashes are shown in Table 1.

The objectives of this "open" literature review are to describe the various concepts and techniques that have been used in the satellites listed in Table 1, to evaluate their experimental data, and to assess, if possible, their respective

TABLE 1

Satellites that Detected Lightning

Satellite	Launch Date	Orbit Altitude	KM	Inclination Degree	Period Minutes	Sensors Photometers Angstroms, A	Radiometers MHz
Lofti I (NRC)	May 1961	Apogee Perigee Circular	960 166	27.37	95.9		.018, 4.01, 6.975
Alouette Canadian	Sept. 1962	Apogee Perigee	1031 996	80.4	105		0.4 to 11.5
Ariel II British	March 1964	Apogee Apogee	1360 290	51.67	101		0.5 to 3.5
OSO-B2 U. of Minn.	Feb. 1965	Circular	600	33	96	2800 to 6000	
Vela - B U. of PA Sandia	April 1967	Circular	121030	35	4.6 days		27.7, 34.58, 42.94
Ariel III tish	May 1967	Apogee Perigee	600 500	80	95		5, 10, 15
RAE (1) NASA	July 1968	Circular	5850	121	225		0.2 - 5.4 0.45 - 9
OSO - 5 U. of Minn.	Jan. 1969	Circular	600	33	96	3500 to 8000	
DMSP - 33 DOD	Sept. 1974	Circular	833	98.7	101.56	4000 to 12000	
DMSP - 2 DOD	July 1977	Circular	833	98.7	101.56	4000 to 12000	
ISS-b Japan	Feb. 1978	Circular	1000	70	107		2.5, 5, 10, 25
DMSP - 3 DOD	April 1980	Circular	833	98.7	101.56	4000 to 12000	

efficiencies in terms of the users' operational requirements and research information as shown in Table 2 (Ref. 2).

To achieve these objectives, it is essential first to know the nature and characteristics of the energy radiated from a thunderstorm.

II - Energy Radiated from Thunderclouds

1. General

In this section, the discussion will be limited to properties of the r.f. (3000 Hz to 500 MHz) and the optical-IR (4000 Å to 10,000 Å) electromagnetic energies radiated from thunderstorms, and only to that portion of it which can or should be detected by orbiting and stationary satellites.

The radiation is a consequence of a complex physical process that neutralizes all or a portion of the electrostatic charge residing within the thundercloud. The neutralization process is complex and it consists of a series of lightning flashes or strokes that take place between the thundercloud and the ground, referred to as cloud to ground, and between various locations within the thunderclouds, referred to as cloud to cloud flashes. The cloud to cloud flashes occur more frequently than the cloud to ground flashes. However, the cloud to ground flashes are much more energetic than the cloud to cloud.

The lightning flash is a manifestation of the phenomenon by which some of the electrical energy of the thundercloud is transformed by dissociation and ionization into thermal, kinetic, sound, and electromagnetic (r.f. and optical-IR)

TABLE 2

OPERATIONAL AND ENGINEERING APPLICATION REQUIREMENTS

SUMMARY TABLE

Real Time

USER	GEOGRAPHIC AREA	SPATIAL RESOLUTION		SPATIAL RESOLUTION		EVENT/RATE OR INTENSITY	DIRECTION	SPEED	CLOUD/GROUND OR INNER CLOUD DISCRIMINATION	FALSE ALARM	FAIL TO DETECT
		GOAL	MAX	GOAL	MAX						
Utilities	CONUS	±2 mi	±5 mi	10 min	20 min	Yes	Yes	Yes	No	30%	30%
FAA	CONUS	±3 mi	5 mi	20 sec	1 min in terminal area---- 5 min on route	Yes	5-10°	±2 m/sec	No	30%	5%
Telecommunications	None										
Forecasting	CONUS	±2 mi	±15 mi	15 min	60 min	Yes	5-10°	±2.5 m/sec	Yes	30%	10%
Forest Service Fire Detection	CONUS	250 m	1 km	5 min	20 min	Yes	Yes	Yes	Yes, with continuing current monitor	10%	10%
Forest Service Storm Tracking	Western USA	±2 mi	±5 mi	15 min	45 min	Desirable	--	--	--	30%	10%
US Air Force (Best Estimate)	Worldwide	±3 mi	5 mi	5 min	10 min	Yes	5-10°	±2.5 m/sec	No	30%	10%

Research Information

USER	GEOGRAPHIC AREA	DIURNAL INFORMATION	EVENT RATE	CURRENT WAVEFORMS RISE & FALL TIME & PEAK MAGNITUDE	STORM SIZE	STROKES/ FLASH	SEVERE STORM MONITORING	RATIO OF INNER CLOUD TO GROUND DISCHARGES	RELATIONSHIP BETWEEN LIGHTNING & RAIN
Utilities	CONUS	Yes	Yes	Yes	Yes	Yes	No	Yes	No
Telecommunications	CONUS	No	Yes	Yes	Yes	Yes	No	Yes	No
Forecasting	CONUS	Yes	Yes	No	Yes	Yes	Yes	Yes	Yes
US Air Force	Worldwide	Yes	Yes	Yes	Yes	Yes	No	Yes	No
FAA	CONUS	No	No	Yes	No	Yes	No	Yes	No
Forestry Service	CONUS	No	No	No	No	No	No	No	Yes

Source: NASA Report No. CP-2095, July 1979
Reference: (2)

energies. Specifically. it is a narrow channel of a high density of excited and ionized molecules and atoms that exists for a short interval of time between the base of a thunder-cloud and the earth or between the oppositely electrical charged centers within the cloud. The ionized channel provides the conduit by which the negative charge at the base of the cloud is neutralized by the flow to it of the positive charge from the earth. As a consequence, a current of approximately 10^4 amperes flows through this conduit for a very short time (microseconds), and, as a result, the temperature of the column is momentarily increased to values ranging from $10{,}000^{\circ}K$ to $30{,}000^{\circ}K$, producing further dissociation of molecules and atoms in the channel. The phenomenology of these transformations is discussed by Uman (3), Schonland (4), Israel (5), Chalmers (6), Kitagawa (7), and in the proceedings of the five international conferences on atmospheric electricity (8 - 12).

2. Radio Frequency Radiation (r.f.)

The instantaneous flow and decay of current through the ionized channel produces the electromagnetic energy that is radiated in the radio frequency band; whereas, the association and de-ionization of air molecules and atoms within the channel are responsible for the optical-IR electromagnetic energy. Uman (3), Pierce (13), and Brook (14) present detailed reviews of these physical processes and, also, analyze and interpret the spectra of the electromagnetic radiation.

In Fig. 1, Pierce (13) shows the variation with frequency of the amplitude of the electric field as measured at a

distance of 10 km from the thunderstorm.

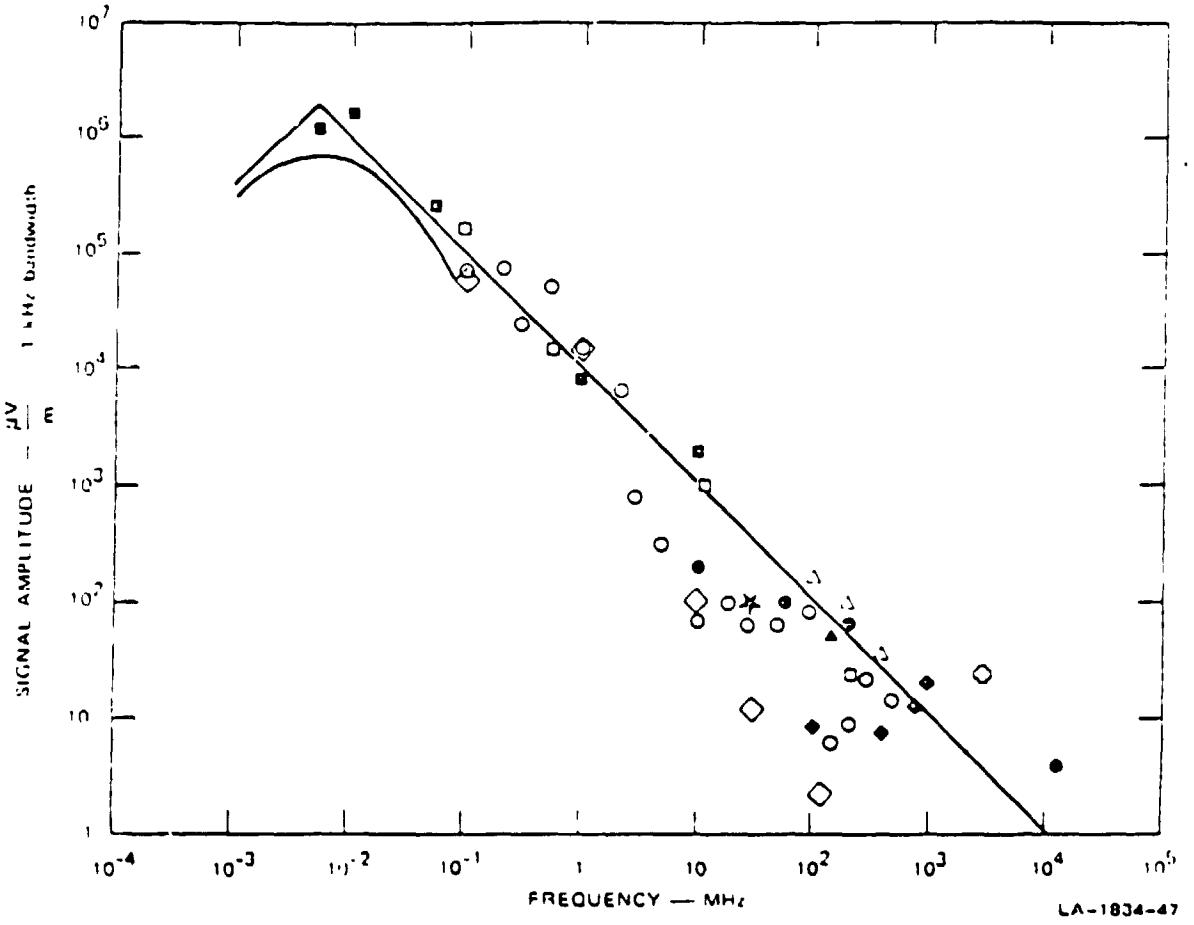

PEAK RECEIVED AMPLITUDE AT 10 km FOR SIGNALS RADIATED BY LIGHTNING

Fig. 1

Source: E. T. Pierce
Reference: (13)

The data on this graph represent the experimental values of many scientists who measured the r.f. radiation produced by various electrical discharge processes in the complete lightning flash. The references for the data points can be found in the paper by Oetzel and Pierce (15). [See also Kimpari (16),

Horner (17), and Horner and Bradly (18).] The spectrum is essentially continuous from 3000 Hz to 500 MHz. However, various discharge processes within the entire period of lightning flash produce different amounts of radiation at different frequencies. The peak signal amplitude is attained at approximately 10 KHz. It decreases by approximately a factor of 10^5 from 3000 Hz to 500 MHz. From 3000 Hz to 5 MHz this decrease is linear; whereas, from 5 MHz to the higher frequencies it decreases more rapidly. Weidman, Krider, Uman (19) measured the spectral amplitudes of the "step leaders", of the positive and negative intra cloud discharges, and of the first stroke (return stroke). They report that at frequencies from 5×10^5 Hz to 5×10^7 Hz the reduction of signal amplitude could vary as f^{-2} to f^{-5} (f = frequency). Since very few measurements were made at these higher frequencies, Brook (14) concluded that beyond 50 MHz the amplitude vs frequency characteristics are not yet clearly defined.

Malan (20) found that amplitude-frequency relationship varied substantially between a cloud to ground and a cloud to cloud discharge. He examined the r.f. radiation from more than 1000 flashes of cloud-ground and cloud-cloud discharges. The differences in amplitudes at different frequencies for both of these types of discharges are shown in Fig. 2.

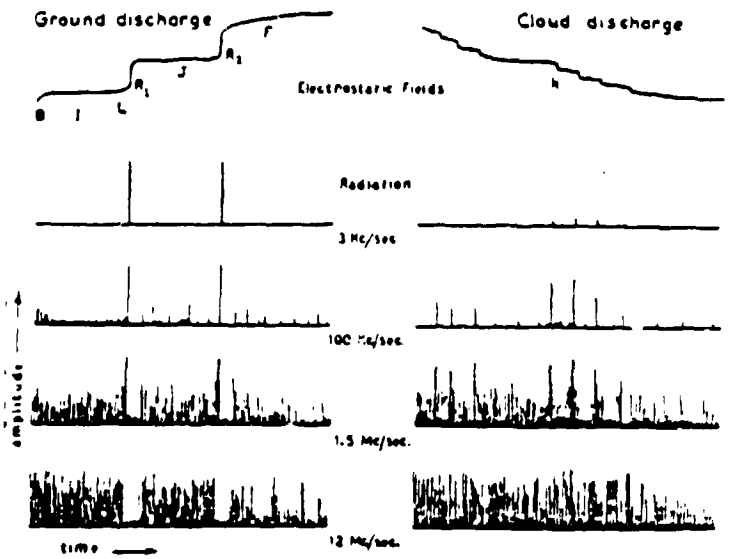

—Diagrams of electrostatic field changes and the corresponding radiation fields at different frequencies of typical ground and cloud discharges. Only amplitudes of radiations at the same frequencies are comparable.

Fig. 2

Source: D. J. Malan
Reference: (20)

Examination of Fig. 2 reveals that at 3 KHz the amplitude ratio of the cloud to cloud radiation appears to be 20 to 1 to 40 to 1 of that of cloud to ground. At higher and higher frequencies the ratio decreases, approaching unity at 1.5 MHz.

Kimpari's (16) values for these variations are shown in Table 3. These values are an estimate of the relative amplitudes of the respective radiation from ground and cloud flashes in the same frequency band.

TABLE 3

Ratios of the Amplitudes of Return Stroke Radiation of Ground Discharges to Amplitudes of the Most Intense Radiation Components of Cloud Discharges at Different Frequencies

Frequency	Ratio
3 KHz	20/1 to 40/1
6 KHz	10/1 to 20/1
10 KHz	10/1
20 KHz	5/1
30 KHz	2/1 to 3/1
50 KHz	1/1 to 1.5/1
1/5 to 1.2 MHz	1/1

It is to be noted that Malan considered only the most intense radiation produced by cloud-cloud discharges. The ratio values would be undoubtedly much higher if weak cloud-cloud radiation signals had been considered. It is to be noted also that these measurements were made at ground level and at some kilometers distance from the thunderstorm center. Furthermore, as Uman (3) points out, the radiation was detected by tuned circuits, and, therefore, it might be possible that these same circuits could be energized at the same time by other spurious radiation.

3. The Radiation in the Optical-IR Band

The radiation consists of a continuum upon which is imposed a large number of individual and multiple spectral lines. The spectral lines are produced by the ionization and de-ionization of nitrogen, oxygen, and hydrogen, and many more minor constituents. A chronological history and bibliography on the discovery, on the theory, and on the measurement of these numerous spectral lines are presented by Uman (3).

The optical radiation from return strokes is by far the most intense. It is easily identified. T. R. Connor, as quoted by Brook (14), provides quantitative data on the ratio of the electrical energy deposited into the channel to the optical energy radiated by the return strokes and measured at various distances from the strokes. Connor computed the efficiency of conversion. A summary of these values are given in Table 4.

TABLE 4

CALCULATION OF EFFICIENCY.

Stroke Type†	Range (km)	Rain Transmission	Visible Energy* (joules/meter)	Energy Deposited (joules/meter)	Efficiency (ε)
IRS	10.0	8.7×10^{-3}	2.0×10^{3}	3.3×10^{5}	6.1×10^{-3}
SRS	7.0	3.6×10^{-2}	5.6×10^{2}	5.1×10^{4}	1.1×10^{-2}
SRS	7.0	3.6×10^{-2}	4.2×10^{2}	4.0×10^{4}	1.1×10^{-2}
SRS	7.0	3.6×10^{-2}	5.7×10^{2}	9.0×10^{4}	6.4×10^{-3}
IRS	7.2	3.3×10^{-2}	2.3×10^{2}	3.2×10^{4}	7.3×10^{-3}
IRS	4.6	1.1×10^{-1}	2.2×10^{2}	2.1×10^{4}	1.1×10^{-2}
IRS	4.0	1.5×10^{-1}	5.9×10^{1}	2.2×10^{4}	2.6×10^{-3}

Extinction Coefficient Due to Rainfall = 0.475 km^{-1}.

Weighted Average Efficiency = 0.007 ± 36%.

† IRS = First Return Stroke; SRS = Subsequent Return Stroke

* Corrected for (1) humid-air transmission and (2) estimated rainfall transmission.

Source: M. Brook
Reference: (14)

The values in Table 4 indicate that the conversion of electrical to optical energy is less by a factor of approximately 10^{-3}. Krider et al (21) measured the radiated power in

the band 4000 - 11,000 Å for a single lightning flash to be 6.2×10^6 watts/m. The computed input optical power was 1.1×10^{10} watts. Turman (22) measured the power of lightning flashes (4000 - 11,000 Å) occurring in Florida. He obtained a value of 2×10^9 watts. He commented further that no peak power greater than 2×10^{11} watts was observed.

Simultaneous daytime optica measurements of lightning flashes were made by Brook et al (23) at approximately 20 km above and 20 km distance from a thundercloud. An optically instrumented U-2 was used to make the measurements above the clouds. A duplicate optical system was used on the ground, in this instance, at the Langmuir Laboratory in New Mexico. The calculated values of 21 pulses measured at the U-2 altitude of 20 km are listed in Table 5.

TABLE 5

Measured optical pulses at U-2 altitude and calculated equivalent source peak power

Pulse #	Measured Output Voltage (mV)	Calculated Equivalent Source Strength (W)
1	28.7 ± 6%	9.3×10^7
2	20.7 ± 8%	6.7×10^7
3	18.0 ± 9%	5.8×10^7
4	17.4 ± 13%	5.5×10^7
5	44.8 ± 6%	1.4×10^8
6	37.4 ± 6%	1.2×10^8
7	30.7 ± 10%	1×10^8
8	38.7 ± 6%	1.3×10^8
9	26.0 ± 6%	8.4×10^7
10	16.7 ± 9%	5.5×10^7
11	19.3 ± 8%	6.2×10^7
12	14.0 ± 11%	4.5×10^7
13	13.4 ± 11%	4.3×10^7
14	60.8 ± 3%	2.0×10^8
15	44.8 ± 4%	1.4×10^8
16	74.8 ± 3%	2.4×10^8
17†	210. ± 3%	6.8×10^8
18†	390. ± 2%	1.3×10^9
19†	670. ± 1.6%	2.2×10^9
20	9. ----	2.9×10^7
21†*	3260. ± 6%	1.1×10^{10}

* Saturated on high gain. The measurement was derived from the low gain channel. This pulse was associated with the second flash recorded by the U-2, and has no ground-measured counterpart.
† Probable return stroke.

Source: M. Brook et al
Reference: (23)

From this table one deduces that the average value of power of the return is approximately 10^9 watts and the power in other discharge processes of the lightning flash ranged from 10^7 to 10^8 watts. These values agree, generally, with those obtained by Krider et al (21) and Turman (22).

It is interesting to note that the values of the power of the return stroke measured at 20 km above the cloud and measured on the ground at 20 to 50 km distant from the cloud

are, for practical purposes, equal, that is, approximately 10^9 watts. This means that the optical radiation emitted by the discharge of the return stroke was subject to the same losses due to absorption, scattering, and reflection as the radiation propagated through the respective intervening atmospheres. The data shown in Table 4 indicates, however, that values of these losses should differ.

Two important parameters to be considered in the monitoring of lightning by satellite are the spectral components of the optical radiation and the rate of rise and decay of the optical pulse. Barasch (24, 25) made a number of ground measurements of the power of specific spectral lines radiated from a single stroke. [See Brook (14) for additional discussion.] Collimated photometers with interference filters were used to record the radiation. The photometers were pointed toward the greatest occurring lightning discharges. The average values of spectral intensities produced by lightning and measured at 4140, 6563, 8220, and 8900 relative to 3914 Å are given in Table 6. (24) The number of pulses which the averages represent are different because not all of the detectors were in operation at any one time.

TABLE 6

Relative Spectral Intensities Produced by Lightning

	Wavelength				
	3914 Å	4140 Å	6563 Å	8220 Å	8900 Å
Spectral Feature					
Lightning[a]	C[b]	C, NI (6)[b]	C[b], H_α	NI(2)	C
Air fluorescence	N_2^+ 1N (0,0)	$N_2$2P(3,7)	$N_2$1P(7,4)	NI(2)	$N_2$1P(1,0)
All pulses	1	1.2 ± 0.5	2.1 ± 0.8	4.8 ± 2.8	0.8 ± 0.4
Samples/storms	-	409/2	842/4	482/3	89/1[c]
First return strokes	1	1.0 ± 0.2	1.2 ± 0.3	1.5 ± 0.6	0.5 ± 0.2
Samples/storms	-	12/2[d]	26/4	30/3[c]	21/1[c]

Notes: a. C = continuum.

b. Slitless spectra show continuum to be present throughout the visible spectrum, producing the main contribution to signals at 3914 and 4140 Å.[1]

c. To increase data sample, some data have been used for which distances were estimated. See text.

d. To increase data sample, some data from a near storm have been used without correction for distance. Estimated error in 4140-Å/3914-Å ratio is small. See text.

Source: G. Barasch
Reference: (24)

The most probable value of the 3914 Å line shown in Table 6 is about 10^4 $Wsr^{-1}A^{-1}$. The total power radiated - using the values shown in Table 6 - is equal to 4.3×10^9 watts.

Brook (14) measured the incident peak spectral irradiances for pulses in the same flash. The spectral irradiances ($Wcm^{-2}A^{-1}$) for eleven pulses are listed in Table 7 (14). The source of this radiated energy was from ground lightning strokes 27 km distant.

TABLE 7

INCIDENT PEAK SPECTRAL IRRADIANCES FOR PULSES
IN THE SAME FLASH, 27 km DISTANT

Time msec	Event	Spectral Irradiance 3914 Å W cm^{-2} A^{-1}	Spectral Irradiance 6563 Å W cm^{-2} A^{-1}	*Ratio 6563 A / 3914 A
-009	(a) 1L	2.0×10^{-12}	7.8×10^{-12}	3.9
000	(b) 1RS	1.1×10^{-10}	5.7×10^{-10}	5.2
040	(c) SRS	1.3×10^{-10}	4.8×10^{-10}	3.7
060	---	1.1×10^{-12}	4.9×10^{-12}	4.5
077	(d) K	2.1×10^{-12}	1.3×10^{-11}	6.2
095	(c) SRS	1.6×10^{-11}	1.1×10^{-10}	6.9
096	(c) SRS	6.4×10^{-12}	4.3×10^{-11}	6.7
125	(c) SRS	2.5×10^{-11}	1.4×10^{-10}	5.6
126	(c) SRS	1.2×10^{-11}	8.6×10^{-11}	7.2
141	(d) K	4.0×10^{-12}	1.9×10^{-11}	4.7
168	(c) 1'RS	9.7×10^{-11}	6.2×10^{-10}	6.4
				Ave. 5.6

Legend
1L = First Leader
1RS = First Return Stroke
SRS = Subsequent Return Stroke
K = K - Change
1'RS = A New Channel 1RS

Source: M. Brook
Reference: (14)

*Computed by the author

The average value of the ratio of the irradiance of the 6563 Å to 3914 Å for all pulses shown in Table 7 is 5.6 as compared to the value of 2.1 shown in Table 6. The difference in these values is indicative of the difference in the chemical composition of the atmospheres in which the lightning occurred and, also, through which the energy is propagated.

The time histories of the various optical pulses are governed by the type of discharges occurring in the thundercloud. The rise time of integrated optical pulse is approximately 100 μ s; whereas, its decay time is approximately 300 μ s. These very fast rise times can be used to discriminate against d.c. and very slow varying background optical radiations.

The above electrical and optical characteristics of lightning are the most important in the design of optical systems for detecting and monitoring global thunderstorm activities. The values of the various parameters are shown in Table 8.

TABLE 8

Source Characteristics of Lightning

1. Peak Power

Return Stroke	$10^9 - 10^{12}$ watts
Subsequent Strokes	$10^7 - 10^8$ watts

2. Electric Field

Signal Strength at 10 km	μV/m
.01 MHz	10^6
1 MHz	10^4
10 MHz	10^3
100 MHz	10^2

3. Optical Power

Relative Spectral Intensities for all Pulses	Barasch (24)*	Brooks (14)*
3914 Å	1	1
4140 Å	1.2	
6563 Å	2.1	5.6
8220 Å	4.8	

4. Time History

	μs
a. Electrical	
Rise Time (return stroke)	0.1 to 10
Decay Time (return stroke)	10 to 50
b. Optical	
Rise Time	100
Decay Time	$\geq$ 300

*Derived by author from data in Table 7

III - Satellite Lightning Monitoring Systems

1. General

In the early 1960s the satellite was envisioned as the principal component of world-wide radio frequency communication and navigational networks. The design and development of the networks required knowledge of the interaction of the communication radio wave and the ionosphere. The study of the interaction is complicated by the "ever-presence" of noise radio waves occupying the same frequency spectrum. Specifically, noise signals in the frequency range from 10 KHz to 500 MHz are a source of potential interference to radio reception in a satellite. The sources of these noise signals are the galaxies, radio transmitters on the earth, and terrestrial lightning discharges. Lightning discharges from thunderstorms could be, however, the limiting factor because the energy radiated by a single discharge is much greater than the energy radiated from any other man-made source.

The radio frequency (r.f.) signals produced by lightning undergo modification, affecting amplitude and phase, as they propagate through the volume of thunderstorms, through the lower atmosphere, and primarily through the ionosphere. In the ionosphere, the signals suffer losses due to absorption, reflection, and refraction. The magnitude of the losses is a function of electron and ion densities in the ionosphere and of its critical frequency.

The scientific missions of the satellites listed in Table 1, page 2, were essentially to study the nature of

these losses. In addition, some of the satellites using electrical and optical techniques, were instrumented to measure the properties of signals produced by lightning flashes. The scientific missions of, the lightning detection systems used by, and the experimental data acquired by these satellites are presented in the subsequent sections.

2. Radio Frequency Systems

2.1 Lofti-1 (Low Frequency Trans-Ionospheric Satellite)

Lofti-1 (Low Frequency Trans-Ionospheric) satellite was the first of the Navy satellites designed to explore low frequency wave propagation in the ionosphere. It was designed as an experiment to determine the magnitude of the propagation loss of VLF (3000 to 30,000 Hz) radio signals traversing the ionosphere. This loss is caused by the absorption of energy as the VLF interacts with the ionized medium, and is a function of the frequency of the VLF, the electron density of the ionosphere, the collision frequency, and the angle of incidence. Most of the loss occurs in the D region, that is, at altitudes between 60 and 130 km.

The system concept of the Lofti-1 experiment is shown in Fig. 3 (Leiphart et al, Ref. 26). It consists of three radio links, one from a shore 30 kw VLF (18 KHz) transmitter to the satellite, one from a shore transmitter to a shore VLF (18 KHz) receiver, and one from satellite to shore UHF (136 MHz) receivers. The shore-based transmitter radiated VLF signals which were intercepted by a 20" diameter loop antenna and a 15 foot long whip antenna. The locations of the antennas

on the satellite are shown in Fig. 4. The VLF (18 KHz) signals were processed by an amplifier, having a band width of 20 Hz. The output was recorded as a peak field strength (microvolt per meter). The processed information was telemetered via an UHF (136 MHz) radio link to various ground receiving stations located around the globe. The UHF transmitter was located at Panama. An example of the type of data received is shown in Fig. 5. (The random short duration "pips" preceding the first time pulse , T1, are identified as lightning pulses.)

During a dawn pass, at a height of 400 km over Central America, and during the daylight part of the pass, several noise peaks due to lightning had values between 10 uV/m and 00 uV/m. In the absence of the ionosphere, it can be shown that a typical 10 Kz signal at the height of 400 km would have an electric field value of 1 mV/m. Leiphart et al (26) indicated that at this particular time the propagation loss through the ionosphere for the 18 KHz signal was approximately 30 db. Applying this loss to the computed 1 mV/m signal, they derived an average value of 32 db for the lightning pulses which is in excellent agreement with the Lofti-1 measured value

The Lofti-1 data indicated that 50% of the time the VLF (18 KHz) signal is reduced less than 13 db at night and less than 38 db by day as it traverses the ionosphere.

The Lofti-1 measurements indicate that VLF signals can and do consistently penetrate the ionosphere. Since peak energy of a lightning discharge lies within the frequency region 8 to 20 KHz, and has value 10^4 times greater than at

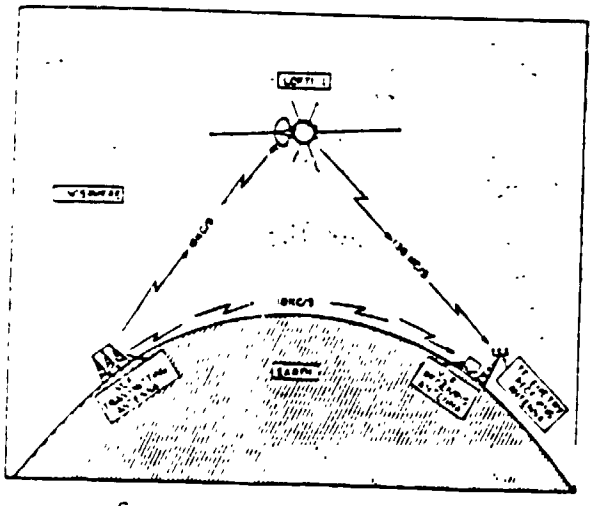

—System concept of the LOFTI I experiment showing the three basic radio links.

Fig. 3

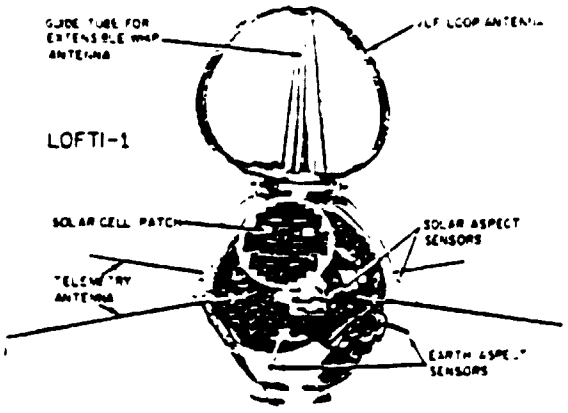

—Side view of the LOFTI I satellite.

Fig. 4

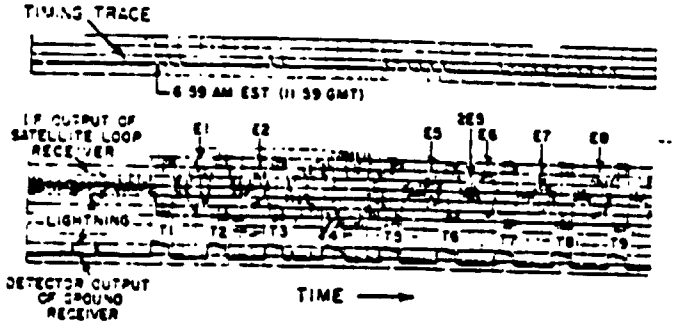

VLF echoes in the ionosphere. Signal output of LOFTI I loop receiver (final IF amplifier). Orbit revolution 434 March 22, 1961, 6:58:58 to 6:59:08 A.M. EST. Satellite off east coast of Florida; height, approximately 385 km; ground range from transmitter (NBA, Panama), approximately 2100 km north. T_1 to T_9 are time pulses of NBA as received by the satellite. E_1 to E_8 are primary echoes of these pulses and 2E5 is probably a secondary echo.

Fig. 5

Source: J. P. Leiphart, et al
Reference: (28)

100 MHz, the VLF techniques could be used to detect and measure lightning pulses. Also, by the addition of three orthogonal loop antennas to the receiving network of the Lofti-1 satellite, the geographical regional location of the source of lightning could be determined. The accuracy, however, would not be adequate to satisfy the requirements listed in Table 2, page 4.

2.2 Alouette Satellite

The primary mission of the Canadian Alouette satellite was to study the absorption properties of the topside of the ionosphere by probing it with pulses of r.f. signals transmitted from equipment on orbiting satellites. The equipment on satellites is referred to as a topside ionospheric sounder (27 - 30). The concept was to irradiate the topside of the ionosphere with pulses of radio frequency waves. The power radiated from the satellite transmitter was 10 watts. The frequency of radio waves was varied from 0.4 to 11.5 MHz. They would interact with the ionsphere and be reflected back to the satellite. The reflected pulses were received by two orthogonal dipole antennas, one 150 feet to receive radio signals having frequencies equal to and less than 4.5 MHz, and the other 75 feet for receiving signals from 4.5 to 11.5 MHz. The output of the receivers would be indicative of the magnitude of absorption experienced by the r.f. pulses.

These receivers made it possible to detect r.f. pulses produced by lightning. Horner (17) analyzed the Alouette data acquired over Singapore and Central Africa, over which areas

lightning flashes were recorded by ground-based meteorological instruments. The Alouette did, indeed, detect these lightning flashes. The correlation between the satellite and meteorological data was poor. The Alouette r.f. pulses were too distorted to derive any significant and meaningful conclusions.

2.3 Ariel III Satellite

The detection and the measurement of radio noise produced by lightning require instruments specifically designed for that purpose. The instruments on Lofti-1 and Alouette were not designed to detect lightning; whereas, those on Ariel II and particularly Ariel III were.

The design and the fabrication of the equipment, the scientific missions, the operational requirements, etc., are described in detail in the entire issue of "Proc. of Royal Society", Section A, 311, 1969. It is not the intent in this review to report on all of the engineering, operational, and scientific aspects of Ariel III but solely to confine this review to those aspects pertaining to the measurement of radio frequency noise signals.

The sources of radio frequency noise capable of reaching satellite altitudes are the high power electrical equipment, the radio transmitters operating with fixed frequencies, galactic noise, and lightning discharges. Horner (17) computed the characteristics of the field which would be expected in a band width of 1 kc/s at a height of 10^3 km over one of the main thunderstorm areas if there were no ionosphere. The

results are shown in Table 9. [See Pierce (13) for similar calculations.]

TABLE 9

Estimated Field Characteristics of Atmospheric and Galactic Noise (Height: 1000 km, Band Width 1 KHz)

	Atmospheric Noise in the Absence of the Ionosphere		
Frequency MHz	Amplitude (10^{-6} volts/m) Peak	Ave.	Power Flux Density Watts/m^2
0.01	8000	300	8×10^{-10}
10	11	3	3.9×10^{-14}
100	0.8	0.3	2.4×10^{-16}
500	0.08	0.05	4.9×10^{-18}
		Galactic Noise	
10		0.19	6×10^{-17}
100		0.11	2×10^{-17}
500		0.09	1.2×10^{-17}

One earlier satellite, Ariel II, was launched in March, 1964. It had, among others, a primary mission to investigate galactic and ionospheric noise [Ladd et al (33)]. Its experimental data revealed that a major contributor to total ionospheric noise was lightning discharges. Ariel II provided sufficient evidence that lightning r.f. pulses are measureable at satellite altitude; however, to do so, it is essential to discriminate against the existence of other r.f. noise signals. The experiments on Ariel III were designed to count the number of lightning pulses, to test a particular discrimination technique, and, also, to test a technique to define the source area from whence the r.f. noise pulses originated. In order to

achieve these experimental objectives, it was necessary to include the measurement of ionospheric electron density and temperature, of the distribution of molecular oxygen, of galactic and ionospheric noise, of natural VLF radio, and of h.f. noise from thunderstorms.

The discrimination concept is based on the fact that lightning flash generates a continuum of r.f. energy, the signal amplitude of which varies continuously with frequency. On the other hand, the man-produced noise, such as from radio transmitters, produces discrete narrow band pulses. By using two receivers, tuned to two frequencies, f_1 and f_2, differing in value by 4 KHz or less, it is possible to discriminate against man-made r.f. noise. Examination of the data presented in Fig. 1 shows that the amplitudes of two signals that differ by 4 KHz will be equal. Amplifying these two signals by means of identical r.f. tuned amplifiers will yield output signals that have the same amplitude values. The discrete frequency r.f. pulse, say from a ground-based transmitter, inserted into the receivers, will yield, on the other hand, output signals having appreciable differences in amplitudes. Hence, whenever the amplitudes of the output signals of the two receivers are equal, they indicate that the source of the input signal is lightning. Whenever the two outputs differ in amplitude, the source of input signal could be discrete frequencies radiated by transmitters.

For the Ariel III, the frequencies chosen were 4.998, 5.002, 9.998, 10.002, 14.996, and 15.004 MHz. The reasons

these were chosen were (1) one of the two frequencies may be expected to be somewhat higher than the critical frequency, and (2) the value of the galactic noise is expected to be much less than the value of the noise produced by lightning.

The r.f. noise signals were intercepted by two loop antennas on the satellite. They were mounted on a conical part of the satellite, with their planes orthogonal and intersecting along the spin axis [Harden and Harrison (31)]. One loop was used for 10 MHz receivers and the other for 5 and 15 MHz. Calibrating units were integrated with the receiver system. The receivers were checked during the flight for sensitivity. With the use of loop antennas, the attitude of the satellite had to be know. It was measured independently to an accuracy of $\pm 5^{o}$; therefore, the receiver output could be corrected accordingly.

To minimize the error in counting the pulses, the electronic system was designed to count the average amplitude of the signals when the satellite was orbiting over the thunderstorm and the number of r.f. signals was large. It counted the rms value, when the number of signals was decidedly less; that is, the satellite was at greater distance from the source.

In addition to counting the r.f. signals, the Ariel III concept addresses the problem of determining the geographical location of the source at any given time. It makes use of the interaction of the r.f. signal with the ionosphere.

In traversing the ionosphere, the radio wave is refracted. The degree of refraction is a function of the electron density of the ionosphere and the angle of incidence. For a given electron density there exists a frequency, labelled the critical frequency f_0, of the r.f. wave below which frequency the wave cannot penetrate the ionosphere and above which value it will penetrate and will be refracted. The refraction is governed by Snell's Law. It states that

$$f = f_0 \sec \phi \quad \text{or} \quad \phi = \sec^{-1} \frac{(f)}{(f_0)} \quad (1)$$

where f = frequency of the signal

f_0 = the critical frequency of the ionosphere, and

ϕ = the angle of incidence of signal to the ionosphere

It is obvious the angle of incidence is a monotonically increasing function of radiated energy and a monotonically decreasing function of critical frequency. This means that the satellite should observe noise signals radiated from the sources on the earth on the highest frequencies earliest in time followed by successively lower frequencies as it approaches closer to the source.

The critical frequency, f_0, is proportional to the square root of electron density of the ionosphere, and it varies with season, time of day, and geographical location.

When the observing frequency equals the critical frequency, no penetration occurs even when the angle of incidence is zero or directed vertically upward. The ionosphere, therefore, actually acts as an "IRIS", the aperture of which is governed by the incident angle and the observing frequency.

Stated another way, it is a shield whose shielding function is a function of frequency and incident angle.

Using the fact as expressed in equation (1), and assuming a flat earth and a thin and horizontally stratified ionosphere, and the simplest of geometries, the radius, R, on the earth from which noise energy of a given frequency, f, will reach the satellite at a height, h, is expressed by the formula

$$\frac{(R)^2}{(h)^2} = \frac{(f)^2}{(f_0)^2} - 1 \qquad (2)$$

r.f. signal can only be received from a circular area of radius, R, as shown in Fig. 6 [Horner - Bent (32)].

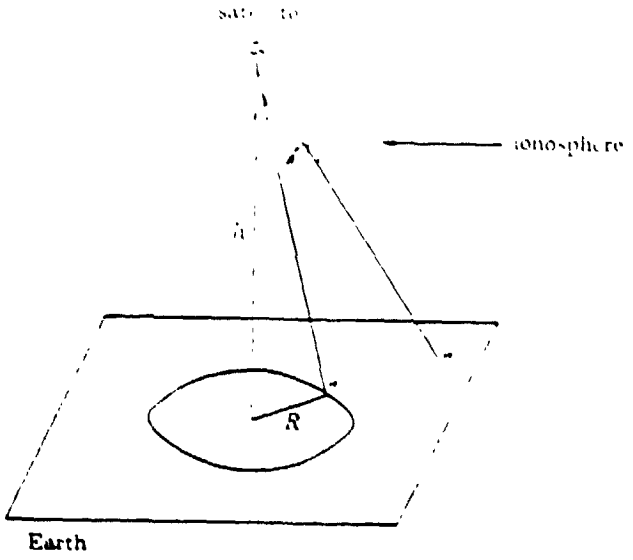

Fig. 6

Area of visibility from satellite (simple theory)

Source: F. Horner and R. Bent
Reference: (32)

Only approximate values of R are computed by the formula. More precise values must consider such factors as angle of incidence, deviative and undeviative absorption, multiple hops, ionospheric tilts, ionospheric inhomogeneity, variability of sferic (RF) amplitudes, etc.

In Table 10, there are computed values of R and of area that Ariel III satellite views on the surface of the earth. In this calculation an average value of 6 MHz was assumed for the critical frequency, f_0.

TABLE 10

Area Viewed by Ariel III

f MHz	R km	A (R^2) $10^6(km)^2$
5	0	0
10	1039	1.08
15	1697	2.87
25	2939	8.41

It is evident from the table that when the frequency of the noise approaches the critical frequency of the ionosphere, the intensity approaches zero.

An example of the radius of visibility as well as of ionospheric absorption is shown in Fig. 7, which represents data taken during orbit 31, May 7, 1967 [Horner and Bent (32)].

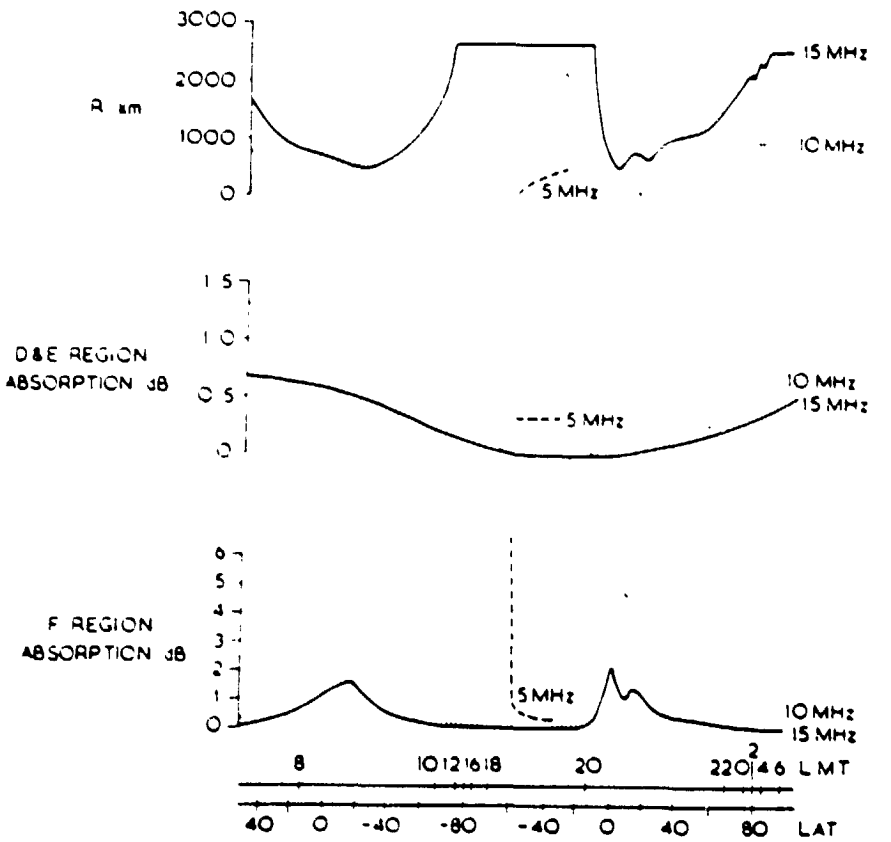

Absorption and radius of visibility for record shown in Figure 4, Orbit 31, 7 May 1967

Fig. 7

Source: F. Horner and R. Bent
Reference: (32)

The computation of the absorption was based on an estimate of electron-height profile, on the collision frequency which varies as electron density, and on the variation of electron density in D and E layers with latitude and local time. If the ionospnere is not horizontally stratified and the critical frequency varies rapidly with latitude and longitude, the atmospheric noise signals can penetrate the ionosphere

in regions of low critical frequencies, after it has been propagated below the ionosphere from a storm in a region where the critical frequency is high. The apparent position of the storm would then be misleading.

The experimental results from a satellite pass over a thunderstorm region of eastern Europe illustrate the detection and discrimination principals. These are shown in Figs. 8 and 9 [Horner and Bent (35)]. It is evident from Fig. 8 that signal amplitudes of the two receivers (10.002 and 9.998 MHz) are equal; hence, the source of these signals can be attributed to lightning discharges occurring in the thunderstorm beneath the satellite. The satellite was passing from north to south (Fig. 9). The first noise signals were recorded at position "A", and the last were recorded at position "B". The ratio of received frequency to the critical frequency shows that the source of noise signal might be located between the two broken lines shown in Fig. 9.

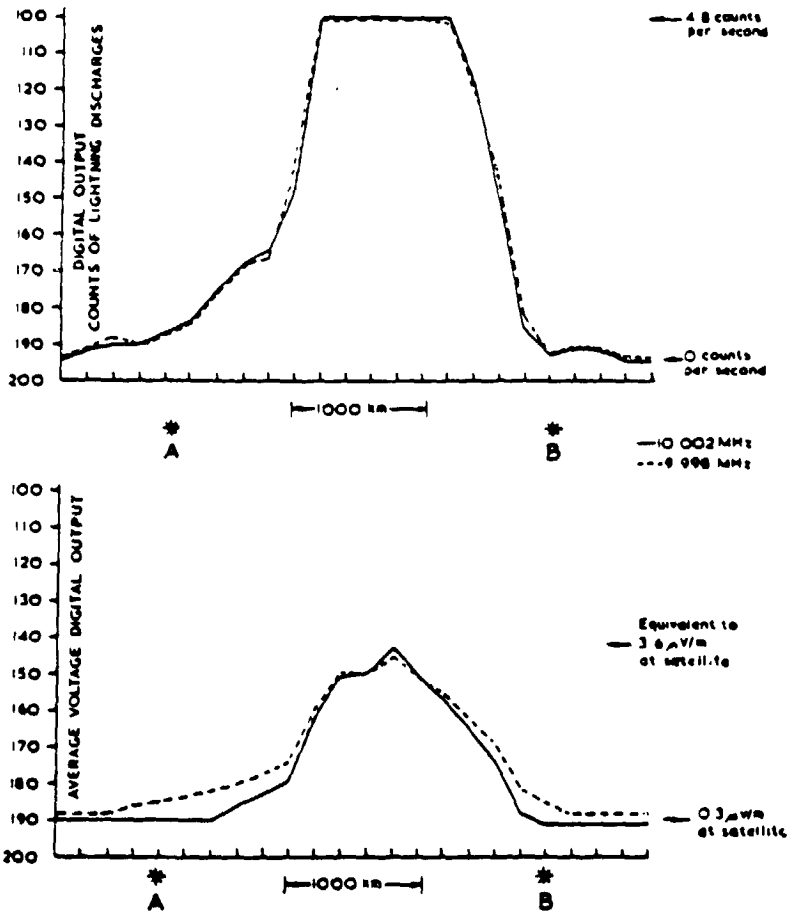

Storm over Eastern Europe July 24 1967, 17.30 U.T.

Fig. 8

Digital Counts of Lightning Discharges
and Average Voltage Output

Source: F. Horner and R. Bent
Reference: (32)

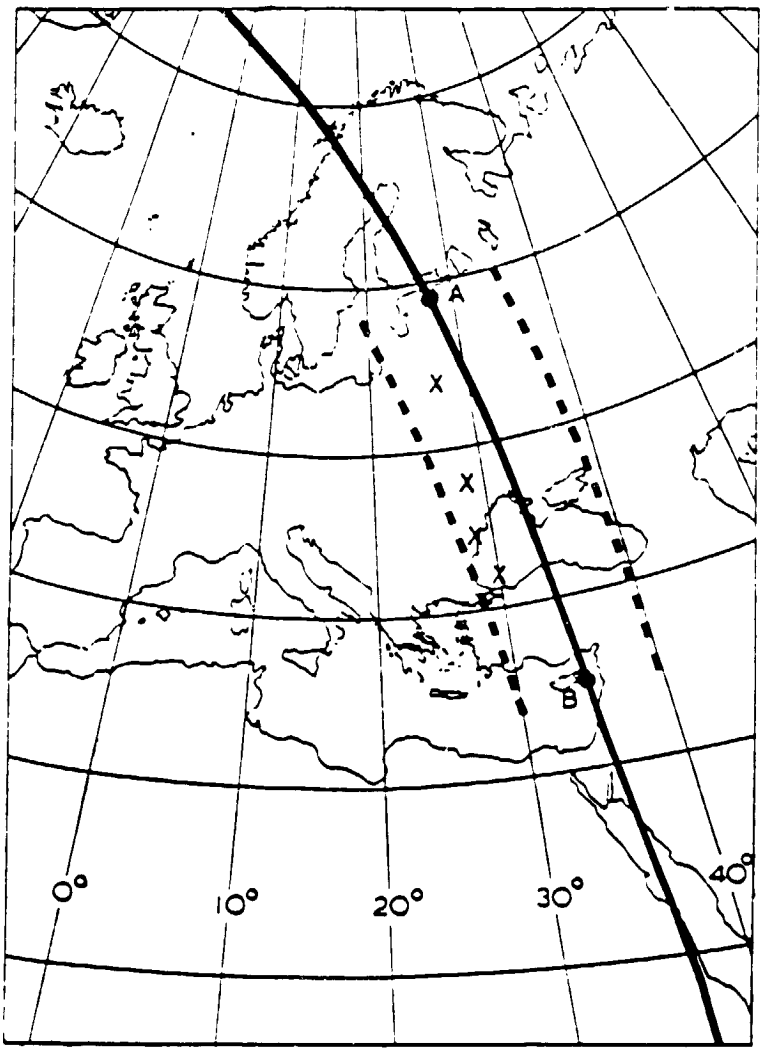

Ariel III pass over Eastern Europe 24 July 1967–17.30 U.T.
(X-storm centres)

Fig. 9

Source: F. Horner and R. Bent
Reference: (32)

Records from the British Meteorological Office taken at the time the satellite passed overhead indicated the presence of storms along this path. The marks "X" indicate the position of the storms at the time. The maximum recorded field strength in the satellite during this period was 3.6 uV/m. The area of the ground viewed by the aerials at the time was $8.3 \times 10^5 km^2$.

In summary, the Ariel III experiments verified the detection concept and the technique to determine the geographical area of the thunderstorm. The discrimination techniques can be improved substantially by adopting in the design of the receivers the latest circuits that enhance selectivity and increase the reduction of extraneous noise signals. The improvement in the location of the sources of noise requires considerably more thought. One idea is to combine the detection concept with an optical system to locate the geographical source. Another idea is to combine the detection concept with a "time of arrival technique" to locate the geographical sources. Undoubtedly, there are many other combinations that can be used.

Assessing the available experimental data of Ariel III, one can only conclude that the concepts and techniques do not provide the accuracy that is needed to satisfy the requirements lised in Table 2. They can, however, be applied to monitor thunderstorms which occur over extensive areas.

2.4 Ionospheric Sounding Satellite (ISS-b), Japan

The results of Ariel III reveal, clearly, that the accurate detection and the counting of global thunderstorm activity by h.f. sensors in satellites require, at any given time, more precise knowledge of the electron density, of electron density altitude profile, of the positive ion concentration, and of the electron and ion temperature parameters that affect the propagation of h.f. signals through the ionosphere. The ISS-b instrumentation includes, in addition to the radio noise (h.f.) measurements, the simultaneous measurements of these parameters. This report will only be concerned with the measurement of high frequency noise (h.f.). [For a description of the measurements of electron density, etc., see Kotaki and Katoh (34) and Kotaki et al (35)].

The mission of ISS-b was primarily to study certain properties of the ionosphere. A secondary mission was to count the radio frequency noise signals produced by terrestrial lightning.

The Ariel III concepts to detect and to determine geographical source of lightning were used in the ISS-b satellite. Four narrow band heterodyne receivers with linear amplifiers were used for detection and discrimination. The ionospheric shielding effect was used to determine geographical location.

The configuration of the components on the satellite is shown in Fig. 10 [Kotaki et al (34)].

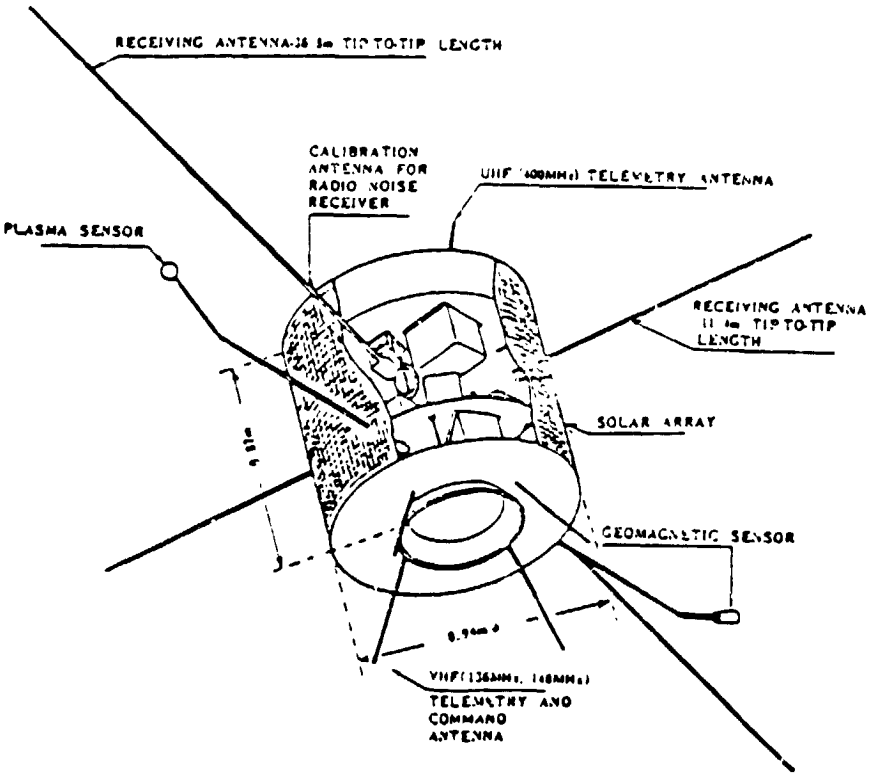

Fig. 10

Configuration of Components on ISS-b

Source: M. Kotaki and C. Katoh
Reference: (34)

The r.f. noise signals were "picked up" by two dipole antennas with lengths of 36.8 m and 11.4 m. These antennas were installed orthogonally on the satellite and were perpendicular to the spin axis of the satellite. The data were transmitted to ground stations via VHF network.

The ISS-b satellite was launched in Japan in February, 1978, into a circular orbit at an altitude of 1000 km with an orbital period of about 107 minutes and with an inclination angle of about 70°. The orbital plane of the ISS-b rotates

westward around the earth's axis by the rate of 3^{o} per day relative to the earth-sun direction, that is, the local time at the satellite position on a fixed latitude shifts behind with the rate of 12 minutes per day.

During the lifetime of ISS-b, it accumulated an abundance of data on lightning. Measurements were repeatedly taken every 64 seconds. The radio noise data were recorded during the first 20 seconds. Since the period of the satellite orbit was 107 minutes, 100 observations of terrestrial r.f. noise were made during one revolution.

The number of noise signals accumulated during every observation period is summarized for every 10^{o} x 10^{o} latitude and longitude of the surface area that is viewed by the satellite. The total number of lightning discharges is normalized by the observation time, and the value obtained is defined as the occurrence rates of thunderstorms. The experimental data acquired were processed by means of a computer.

An examination of Figures 11, 12, and 13 will, as discussed by Kotaki (34) and Kotaki and Katoh (35), reveal the types of radio noise and the effectiveness of the ionospheric shielding concept. Figures 11a, b, c, and d are examples of different types of radio noise signals that were obtained. Each group in Fig. 11 represents the h.f. receiver outputs of Channel 1 (2.5 MHz), Channel 2 (5 MHz), Channel 3 (10 MHz), and Channel 4 (25 MHz). The dotted lines indicate the analog output levels and the crosses the digital counts. The ordinate on the left side of the graphs expresses the analog

Ch. 1
2.5 MHz

Ch. 2
5 MHz

Ch. 3
10 MHz

Ch. 4
25 MHz

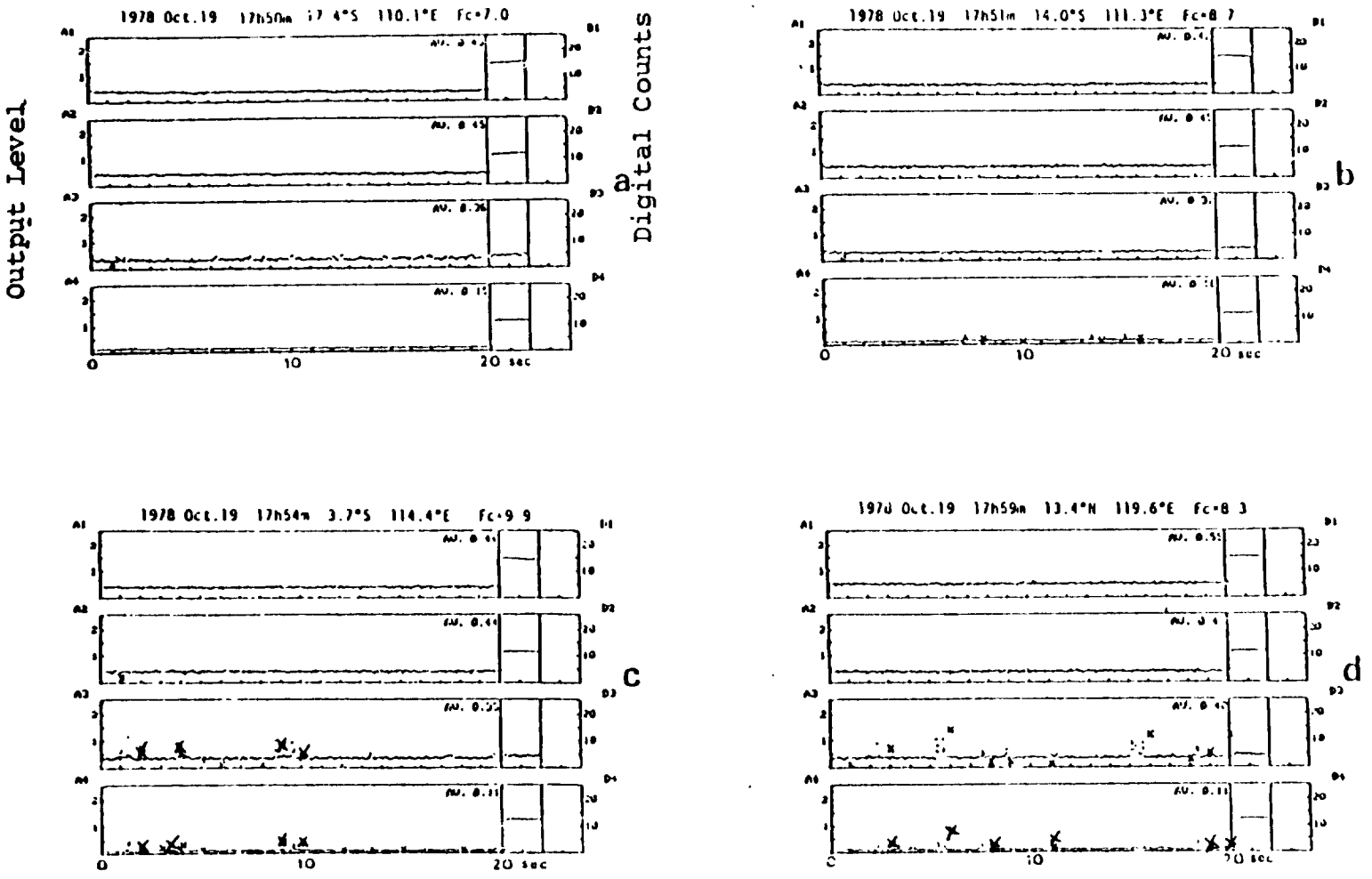

ORIGINAL PAGE IS
OF POOR QUALITY

Fig. 11

Noise Recorded (Oct. 19, 1978) During the ISS-b Pass Shown in Figs. 12 & 13
"X" Indicates Lightning Pulses

Source: M. Kotaki and C. Katoh
Reference: (34)

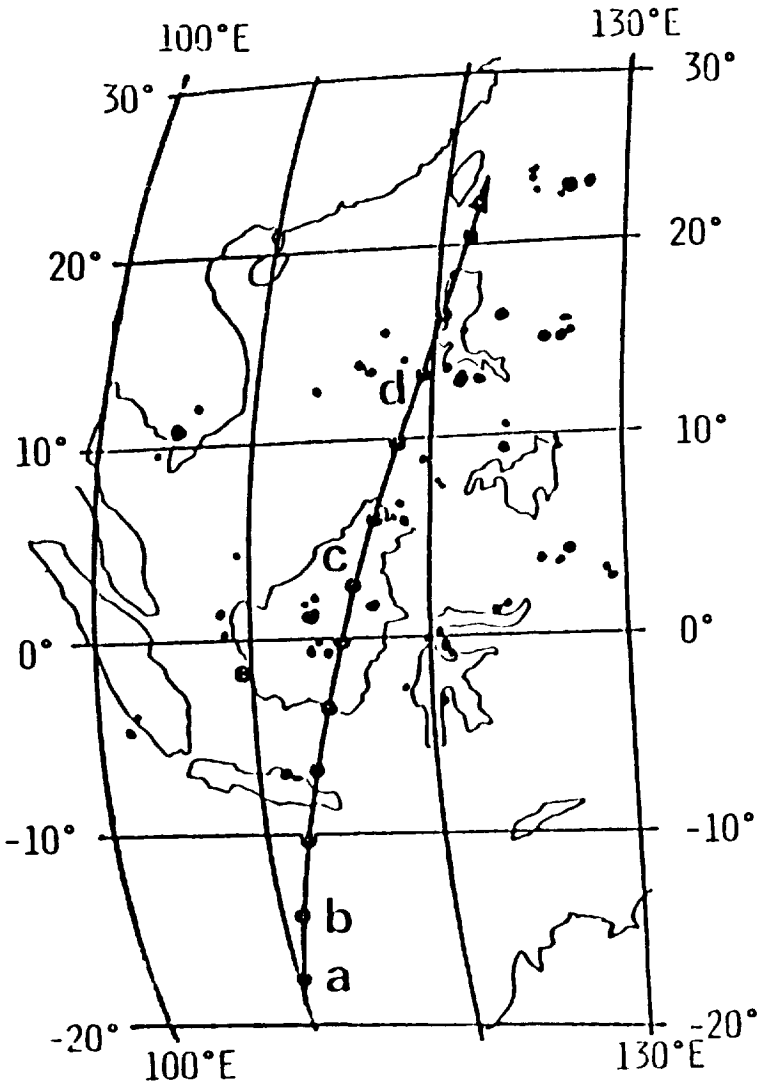

Fig. 12
Ground Trajectory of ISS-b, Oct. 19, 1978

Source: M. Kotaki and C. Katoh
Reference: (34)

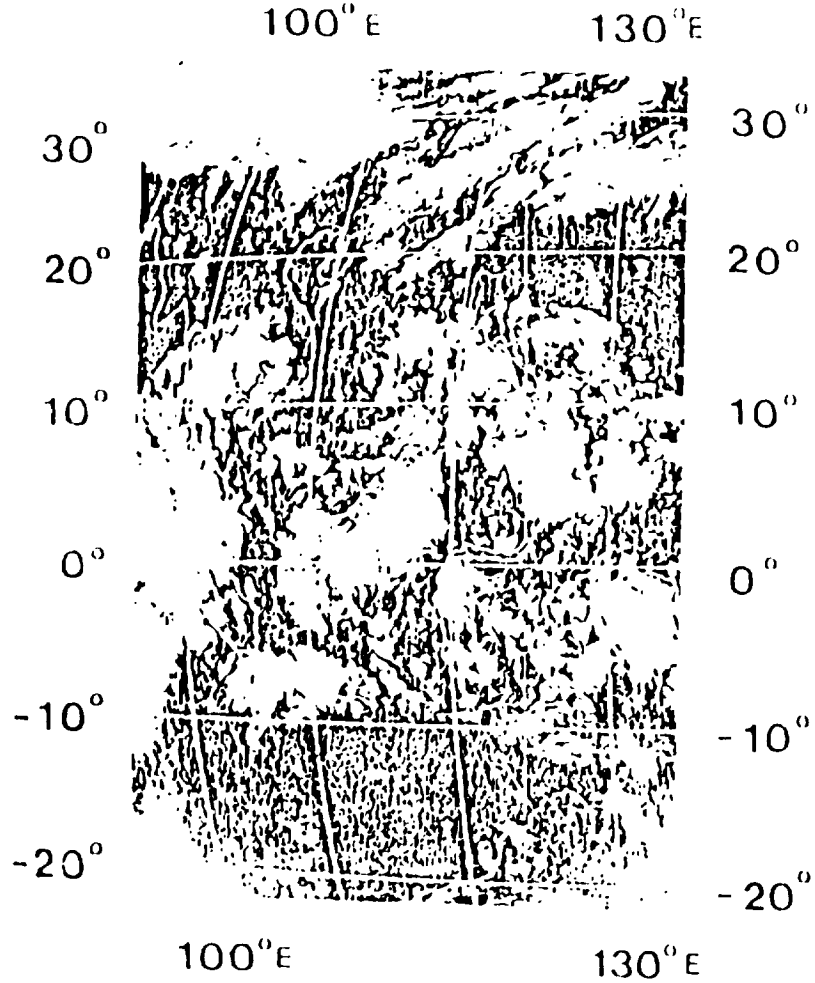

Fig. 13

Infrared Photographic Images Taken by Geostationary Meteorological Satellite
Oct. 19, 1978

Source: M. Kotaki and C. Katoh
Reference: (34)

output in arbitrary units; wher e, the ordinate on the right side expresses the digital output in terms of counts per second.

The lightning pulses detected by ISS-b were compared with the I.R. photographic images of thunderstorm regions acquired by the Geostationary Meteorological Satellite (GMS). The r.f. noises recorded at this time are shown in Fig. 11. The trajectory on the earth of ISS-b orbit and the photographic I.R. image taken at 1800 hr. UT on October 19, 1978, are shown respectively in Fig. 12 and Fig. 13.

Fig. 11 indicates that only galactic noise was recorded in all channels as background noise. This observational result agrees with the fact that no cumulo-nimbus existed around the area concerned.

The radio noise observed at the position "b" (14.0° S, 111.3° E) in Fig. 12 is shown in Fig. 11b. Since the critical frequency of the ionosphere beneath the satellite was 8.7 MHz at the time, according to the relation between f_c/f and R given by the eq. (2), noise signals should be observed at Channel 3 (10 MHz) and Channel 4 (25 MHz) if the lightning discharges occurred within the circular region of radius of about 500 km (f_c/f = 0.87 in this case). As is seen from the observational results shown in Fig. 11, there are some weak increases of analog ouput levels and digital counts at about 8, 10, 14, and 16 seconds in only Channel 4. On the other hand, only the background noise is measured at Channel 3. This fact suggests that the radio waves of the 25 MHz component

emitted from lightning discharges occurred at a distance of 1000 to 2000 km from the sub-satellite point. In this case, there were no thunderclouds over the area surrounding the position "b" of Fig. 12; hence, the atmospherics component corresponding to the frequency of Channel 3 (10 MHz) could not be received because of the "shielding" phenomenon.

The critical frequencies of the ionosphere at the time of observations were 9.9 MHz at the position "c" in Fig. 12 and 8.3 MHz at "d" in Fig. 12. Several bursts of impulsive radio noise are received at Channel 3 (10 MHz) and Channel 4 (25 MHz) in these examples. For reasons stated above, the lightning discharges appear to occur within the circular regions of radius of several hundreds of kilometers centered at the position "c" or "d", respectively. Photograph image, Fig. 13, shows that many cumulo-nimbus existed around the area near "c" or "d" in Fig. 12. Thus, this fact demonstrates indirectly that the impulsive radio noise received by the ISS-b might be emitted from the lightning discharges occurring near the sub-satellite point.

Four lightning discharges are received at the position "c" in Fig. 12 and six lightning discharges are received at "d" in Fig. 12 as seen in Fig. 11c and Fig. 11d, respectively. Since the critical frequencies of the ionosphere beneath the satellite at the position "c" and "d" in Fig. 12 are 9.9 MHz and 8.3 MHz, respectively, the fields of view at "c" and "d" are restricted within the circular area of radius about 130 km and about 500 km, respectively. Therefore, lightning frequencies

per unit area at "c" and "d" become to be about 1.2×10^{-5} $sec^{-1}km^{-2}$, and 1.2×10^{-6} $sec^{-1}km^{-2}$, respectively. These results are in good agreement with Horner's (17) estimation that the lightning frequency per unit area counted by lighting flash counters operating in HF band was about 10^{-5} $sec^{-1}km^{-2}$ at the time of maximum thunderstorm activity.

The above cited illustrations demonstrate the efficiency of the h.f. concept to detect terrestrial lightning. The results of ISS-b indicate convincingly that terrestrial lightning that occurs outside the area as defined by equation (2) will, in all probability, not be detected. Since the defined area is a function of the critical frequency, the ISS-b data also reveal that the detection will be governed by the time of and location (latitude) occurrence of the thunderstorm.

Kitaki and Katoh (34) found that the global frequencies of lightning discharges for the four seasons are about 64 sec^{-1} in the northern spring, 55 sec^{-1} in the northern summer, 80 sec^{-1} in the northern fall, and 54 sec^{-1} in the northern winter. These results are about two times as many as that of Turman's result of 30 sec^{-1}. They also found that, based on 34 impulses attributed to lightning discharges, the peak power flux was 1.4×10^{-13} W m^{-2} $(KHz)^{-1}$. This value is comparable to the value of 3.2×10^{-13} W m^{-2} $(KHz)^{-1}$ derived by Horner for the altitude of 1000 km. Kotaki and Katoh (34) deduced that peak r.f. power radiated by terrestrial lightning varied inversely as $(frequency)^{2.3}$. This relationship differs from

the data shown in Fig. 1 which show radiated power (amplitude of signal shown on the graph) varies inversely as frequency, and it also differs from Weidman, et al (19) who found that peak power varied as f^{-1} from 10^4 to 10^6 Hz and as f^{-2} from 10^6 to 10^8 Hz.

These differences reveal that the relationship between radiated power vs. frequency is actually not known. More experimental data are required before it can be accepted explicitly.

The ISS-b experiment shows that global lightning discharges can be observed by using h.f. receivers in satellites. However, it also reveals that the accuracy of the number of counts and of the locations of the sources of lightning are poor. Interference from ground transmitters affected 30% to 50% of all the data. This interference introduces a large uncertainty in the data. The spatial resolution is also very poor because the condition of the ionosphere plays a major role in the computation. The computations of scanned circular area by ISS-b are more accurate than Ariel III because ISS-b measured simultaneously the value of f_c.

2.5 Vela 4B Satellite

The mission of the Vela series satellites was military in nature. The instruments on board did detect and record pulses produced by lightning flashes. Some of the r.f. data acquired by Vela B satellites was made available to those interested in the detection of lightning flashes.

Vela 4B was launched into a nearly circular orbit with a radius of 19 R_E (earth radius), inclination 35°, and a period of 4.6 days.

Chiburis and Jones (36) analyzed the VHF differential-group-time delay data acquired by the Vela 4B satellite during a pass over the geographical region bounded by 10° to 35° North latitude and 55° to 135° West latitude. The purpose of the analysis was to test applicability of the differential-group-time concept to severe storm identification and location.

The differential-group-time delay concept utilizes the dispersive effects inherent when electromagnetic waves are propagated through the ionosphere. Lightning discharge produces a spectrum of electromagnetic waves, extending from 3 KHz to 100 MHz. The higher frequency waves, 10 MHz to 100 MHz, propagate through the ionosphere. As a group of waves, the lower frequency waves experience a longer group path delay than the higher frequency components. These various delays are calculable if the electron densities are known along the path of propagation. The differential-group-time delay, Δ t, can be approximated by the relation

$$\Delta t = 1.35 \times 10^{-7} \frac{f_2^2 - f_1^2}{f_1^2 \quad f_2^2} \sec\phi \int Nds \qquad (3)$$

where f_2 and f_1 are the center frequencies of the higher and lower of a receiver channel, ϕ is the "look" angle which is the complement of the elevation angle, and $\int Nds$ is the total electron content of the ionosphere. A variation of two

differential-group-time delays as a function of total electron content and the "look" angle are shown in Fig. 14. It is to be noted that the group delays increase with increased electron content and "look" angle.

In order to utilize the "group-delay" concept to detect terrestrial lightning r.f. pulses and to discriminate against the other type r.f. signals elaborate electronic circuits were used. (Details on the circuitry are not available in the open literature.) Two monopole antennas were used to collect the noise signals and to feed them through a passive RLC filter network to each of the VHF receivers. The antennas were located on the satellite in a plane perpendicular to the direction of the earth rotation at an angle of 60^{o} to one another.

To measure the group delays three VHF and one UHF receivers were used in Vela 4B pair of satellites. The typical receiver has four r.f. stages, each with a gain of 20 db, followed by a detector and video output stage. The VHF receivers have center frequencies of 27.70 (Channel "A"), 34.58 (Channel "B"), and 42.94 (Channel "C") MHz. The receiver band widths varied from 1 to 2 MHz.

The satellite data of Vela 4B indicate that r.f. radiation produced by lightning was weakly identified and was not accurately located. The difference in the number of thundery regions that were identified with those that were actually identified by ground measurements was great.

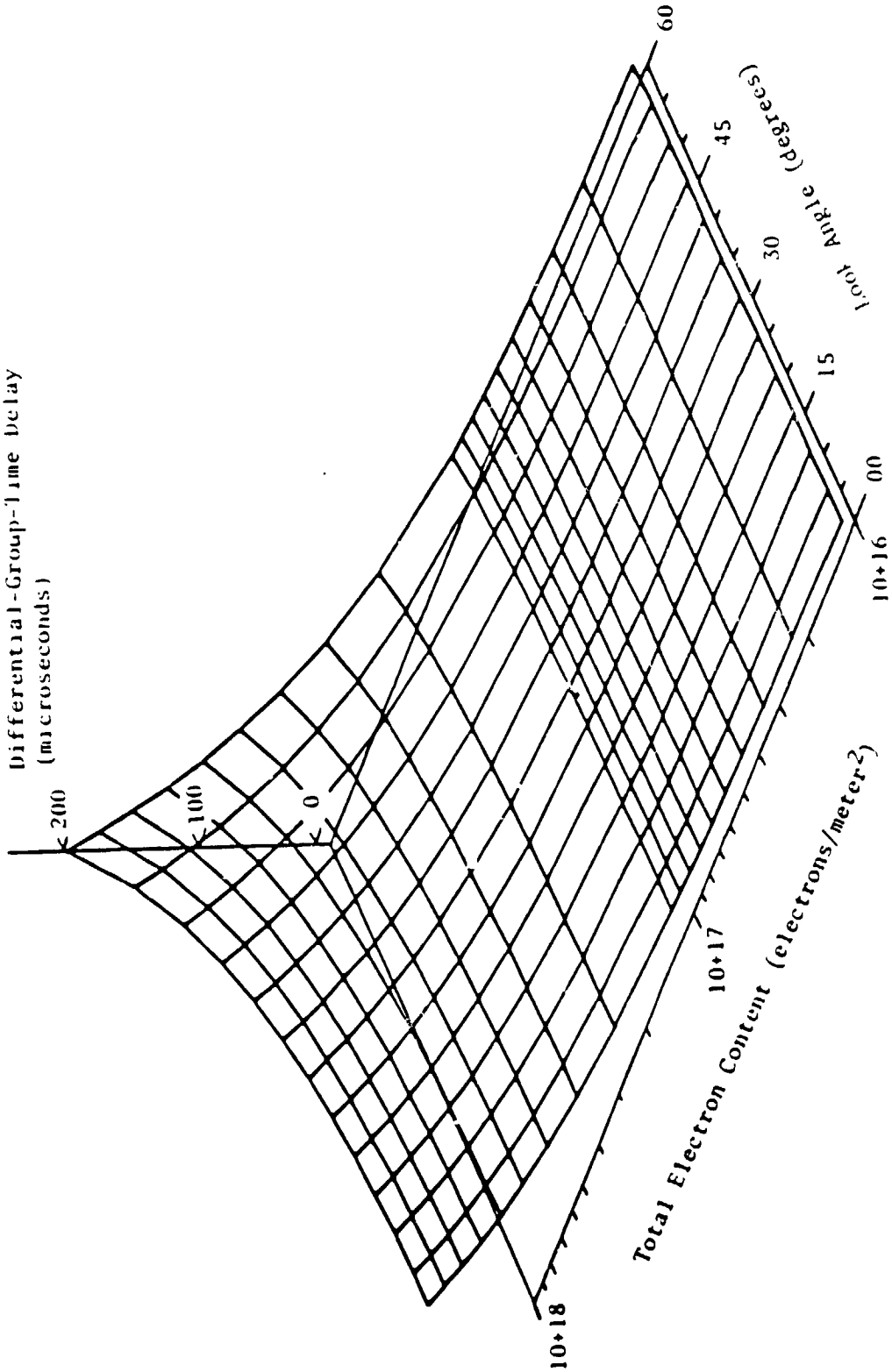

Differential-group-time delay between Channels A and B as a function of total electron content and look angle.

Fig. 14

Source: R. Chiburis and R. Jones
Reference: (36)

At best, the results of Vela 4B indicate that the pulses produced by lightning can be discriminated from other noise pulses by the studious application of the differential-group-time delay concept.

2.6 Radio Astronomy Explorer (RAE-1) Satellites

The mission of RAE-1 was primarily to investigate scientific problems related to astronomy. Since its instrument package included tuned r.f. receivers that covered the frequency range from 0.2 to 10 MHz, it intercepted and recorded terrestrial and galactic sources of radio noise. Herman, et al (37) analyzed the RAE-1 data in order to establish the spatial, temporal, and frequency characteristics of the terrestrial radio noise at an altitude of 6000 km.

In their analysis, they made use of the refractive property of the ionosphere to develop a detection concept which differs somewhat from the one discussed by Horner (17).

The refraction of a radio wave traversing the ionosphere is governed by Snell's Law as formulated in equation (1). Examination of equation (1) reveals that the higher frequencies of the radio waves will be refracted less than those of lower frequencies. Therefore, an orbiting satellite will detect first the higher frequency waves followed by the lower frequency.

The refraction of a radio wave traversing the ionosphere is a function of its frequency and of the critical frequency of the ionopshere, which, in turn, is a function of its electron

density. It also varies diurnally with the height of the ionosphere and with latitude and longitude. The value of the critical frequency can, therefore, be computed or predicted for a given time and geographical location.

Fig. 15 (37) is an example of the variation of the critical frequency. It depicts the critical frequency for 10 hours universal time (UT) and 12 UT in December, 1968. The position of the twilight line separating day from night for these two times is shown as a dashed line. The solid line which is superimposed on this map is the orbit of RAE-1. Gross features of diurnal and latitudinal variations in f_0f_2 (f_0f_2 is referred to the critical frequency of the F_2 layer in the ionosphere) are evident in the contour maps, and as the subsolar (noon) position shifts from 30° E longitude to 0° between 10 UT and 12 UT, so does the twilight line shift in the same direction. Also, the region of minimum value of the critical frequency shifts likewise. It is obvious that prediction of maps of critical frequencies can be used as qualitative guides in determining the extent of ionospheric shielding and distribution of terrestrial radio noise.

An illustration of the combined effect of the ionospheric shielding and terrestrial noise distribution is shown in Fig. 16, where the noise signals, measured as antenna temperatures for the frequencies 9.18, 6.55, 4.7, and 3.93 MHz are plotted as function of time for orbital period 00 UT to 0430 UT, December 2, 1968. Examination of the sequence of times at which RAE-1 received each frequency in the raw

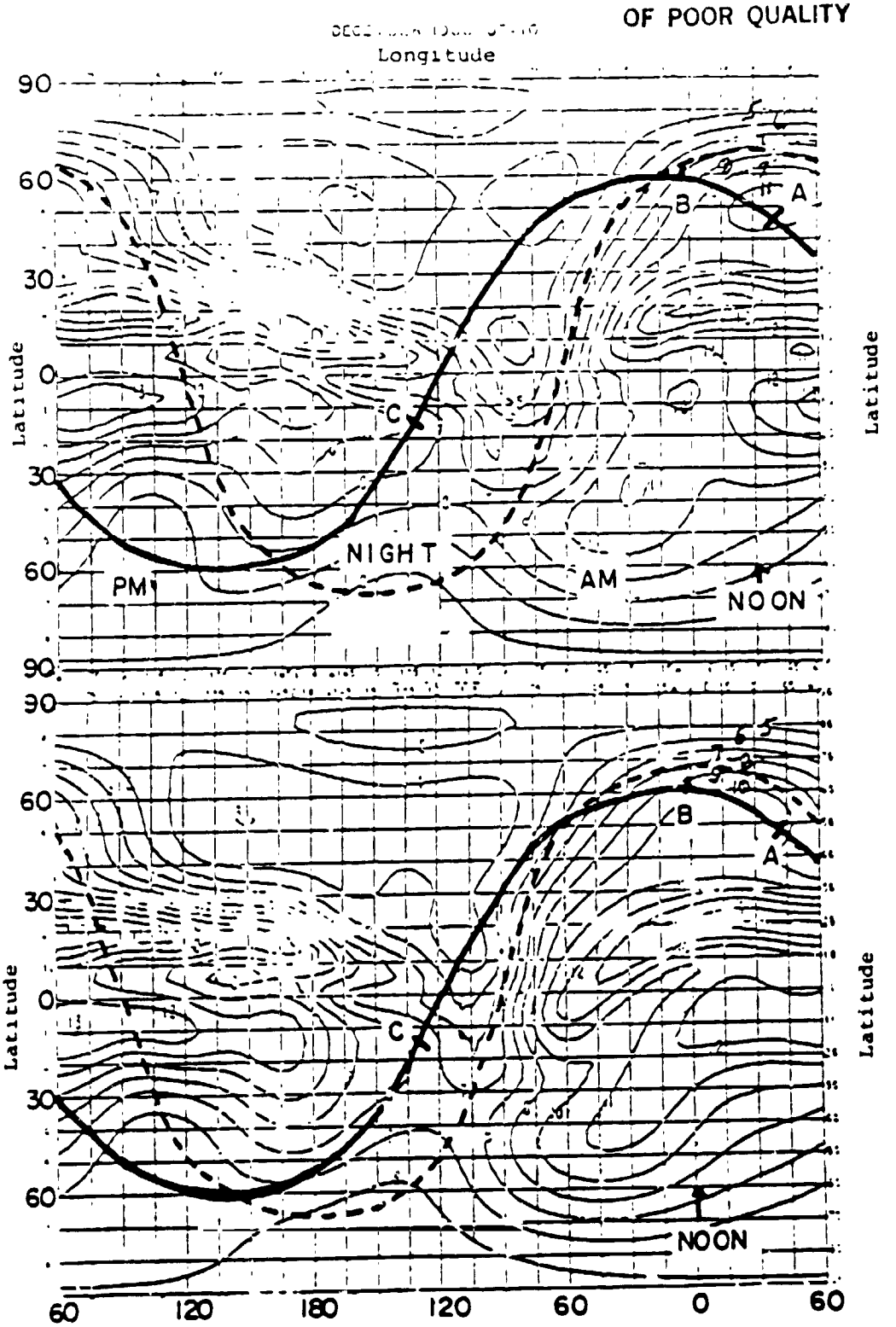

Predicted median foF2 (MHz) for December 1968 10 UT (Top) and 12 UT (Bottom) (After ESSA, 1968). The RAE I orbit is for December 2, 1968 showing satellite positions at 1006 UT (Point A), 1021 UT (B) and 1130 UT (C).

Fig. 15

Source: J. R. Herman, et al
Reference: (37)

ORIGINAL PAGE IS
OF POOR QUALITY

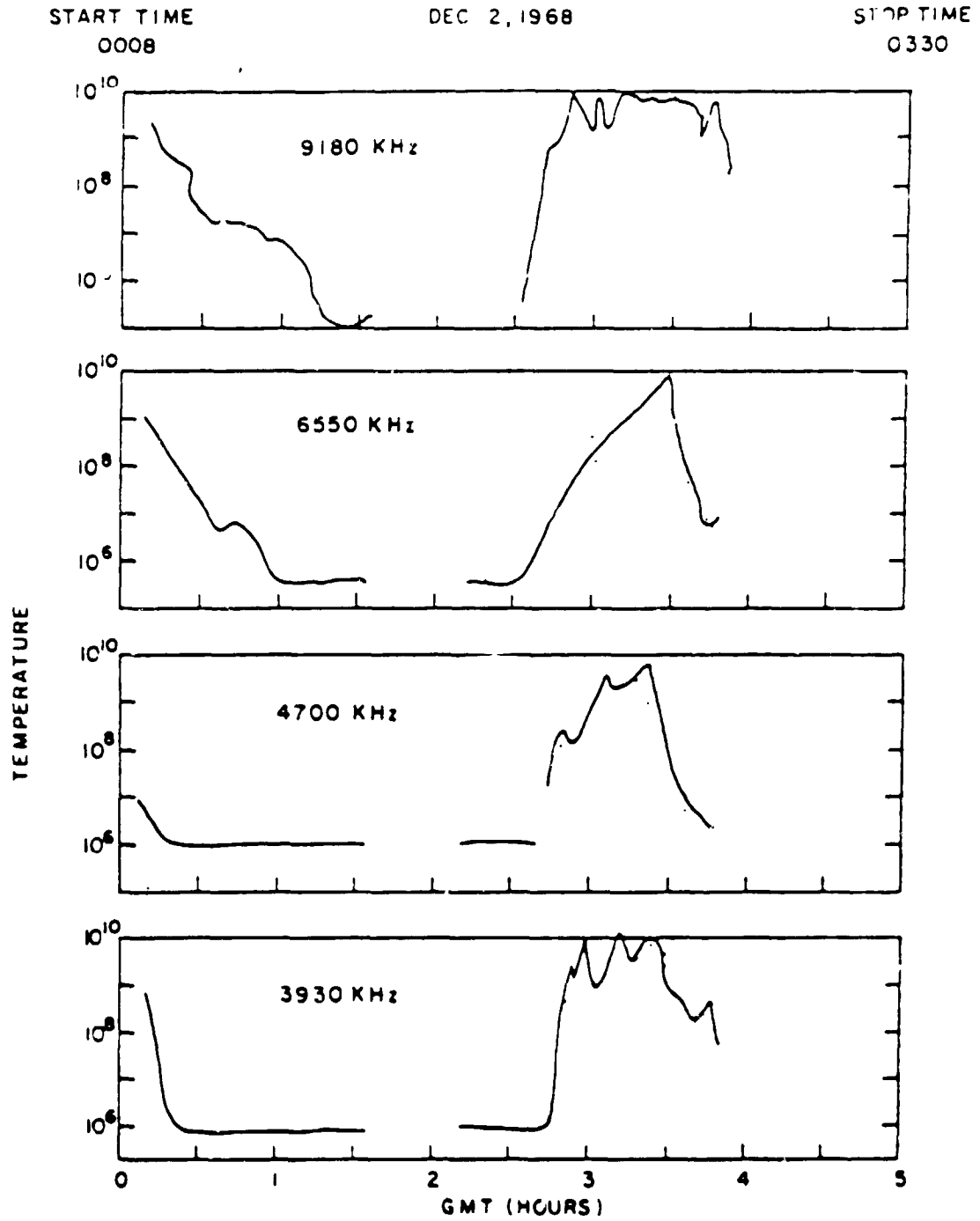

GMAG LAT	1	-32	-48	-30	2	34	48	27	-6	-39	-50
LMT	37	19	217	172	153	132	82	46	28	03	18.8

Full orbit temperature variations measured by lower Vee antenna on 3.9 MHz, 4.7 MHz, 6.55 MHz, and 9.18 MHz. RAE-1 Satellite

Fig. 16

Source: J. R. Herman, et al
Reference: (37)

clearly reveals the shielding effect; ie., 9.18 MHz is received at 0230 UT, followed by 6.55, 4.7, and 3.93 MHz at 0240, 0244, 0246 UT, respectively.

To illustrate the concept, Herman et al (37) computed the radii R_1 and R_2 for frequencies 6.55 MHz and 9.18 MHz, respectively, using equation (1) and the following equation:

$$R_2 = R_1 + \Delta t \, Vg \qquad (4)$$

where t is the time delay between penetration of 9.18 and 6.55 MHz

and Vg is the velocity of subsatellite point along the surface of the earth

From Fig. 16 it is evident that the 9.18 MHz penetrated the ionosphere at 0230 UT, whereas 6.55 MHz penetrated at 0240 UT. This yields a Δ t = 10 minutes. The velocity, Vg, of the sub-point of RAE-1 was 179 km/min. The computed value of R_1 = 1274 km and of R_2 = 3064 km.

RAE-1 was launched in July, 1968, into a nearly circular orbit at an altitude of approximately 6000 km, with an inclination of 121°, and a period of 3 hours and 45 minutes. This orbit allowed the satellite to cover geographical latitudes 59° S to 59° N.

The satellite is equipped with a 37 meter dipole antenna coupled to a burst receiver which sweeps continuously through the frequency range from 0.202 to 5.4 MHz. In addition, it is equipped with two Vee antennas coupled to two Ryle-Vonberg (RV) receivers operating at fixed frequencies from 0.45 to 9.18 MHz. The beam width at frequencies of 3.93, 4.7, 7.55, and 9.18 MHz are respectively 23° x 52°, 15° x 46°, 14° x 36°, and 13° x 27°. The antenna configuration is shown in Fig. 17.

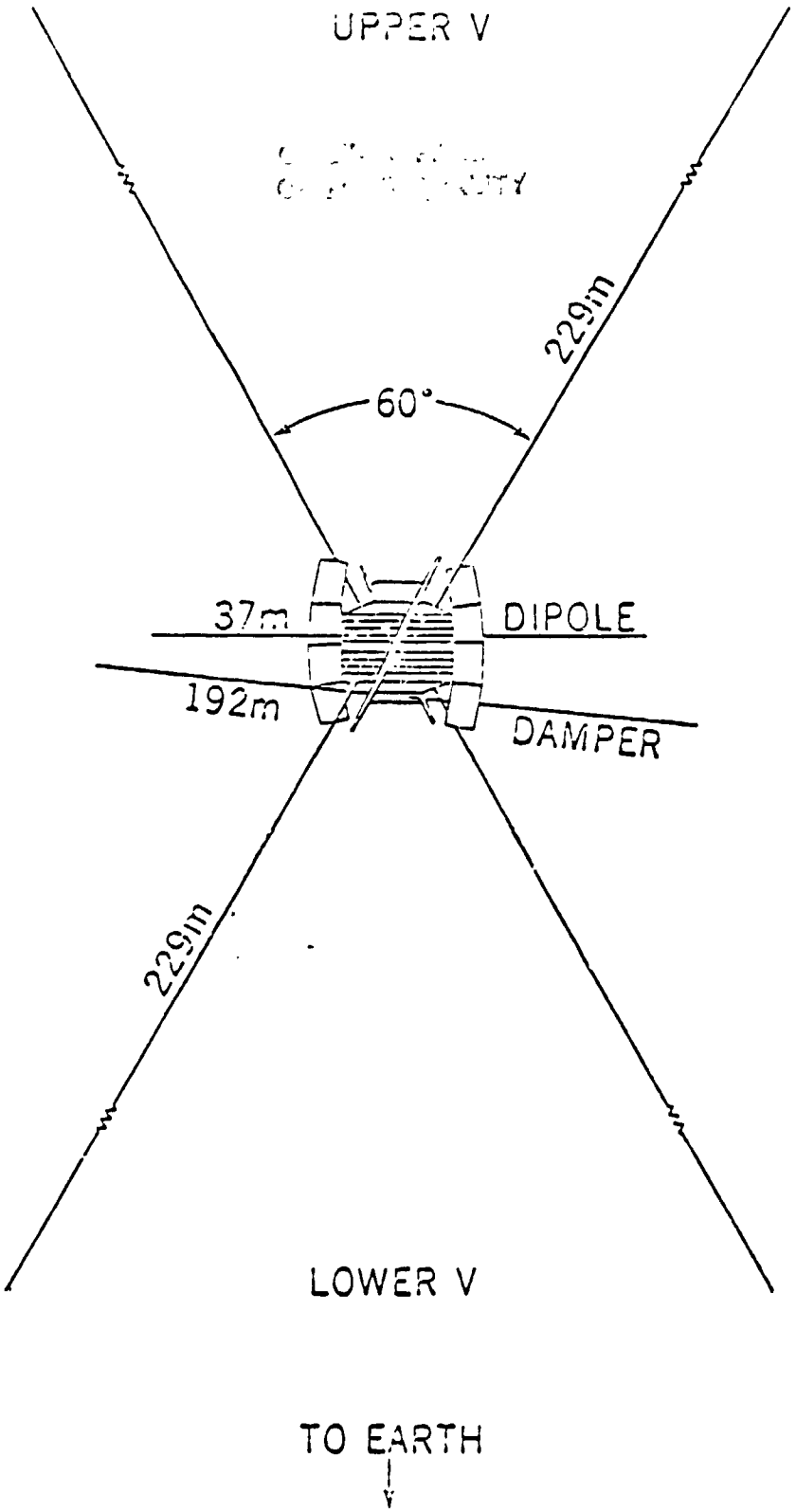

RAE-I Antenna Boom Deployment.

Fig. 17

Source: J. R. Herman, et al
Reference: (37)

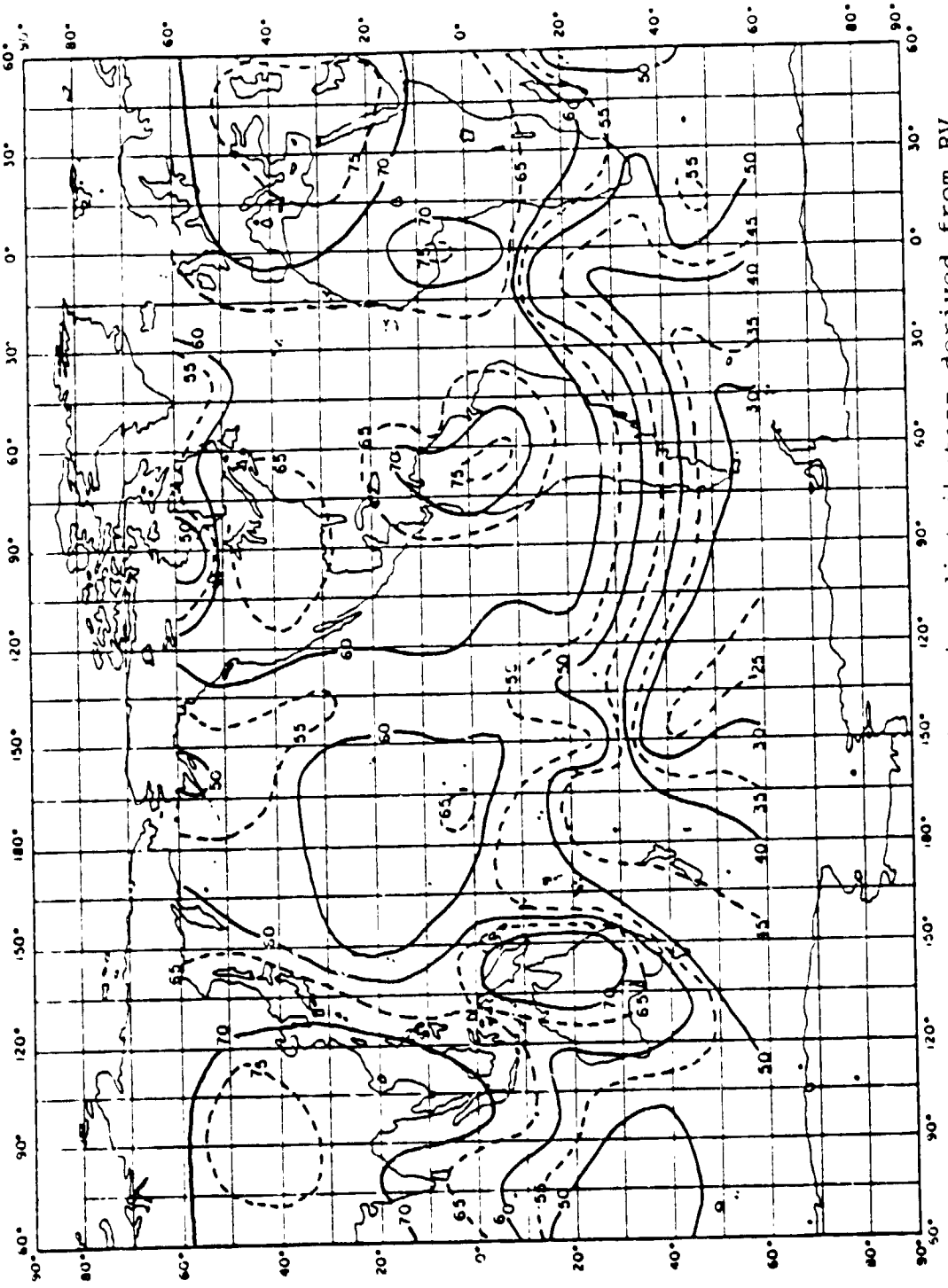

Terrestrial Radio noise distribution derived from RV lower Vee data on 9.18 MHz for Dec. 2-6, 1968, 0000 - 0800LT (Approx. 120 data points). Contour levels are dB above 288°K. RAE-1 Satellite

Fig. 18

Source: J. R. Herman, et al
Reference: (37)

The main lobe of the bottom Vee antenna and back lobe of the top Vee antenna always view the earth, whereas the back lobe of the bottom antenna and the front lobe of the top antenna view outer space. The orientation of antennas allows the determination of the noise arrival direction so that the contributions of various sources may be separated.

Fig. 18 depicts the radio noise distribution derived from RAE-1 data on 9.18 MHz for December 2 - 6, 1968, 0000 - 0800 UT. Counter levels are dB above 288° k. It is evident from these curves that the most intense noise is observed over the major land masses, while the lowest noise levels are over the oceans. Most of the high (70 dB or greater) noise levels are in good agreement with the values found by OSO-5, DMSP, and Ariel III.

The concept of sequential penetration of the ionosphere could be used to define the region a little more precisely than that provided by the use of equation (2). However, this improvement in area definition could be achieved only by the use of a more complex data processing system.

3. Optical Systems

From February to October, 1965, nighttime lightning storms were first observed by the Orbiting Solar Observatory (OSO-2B) satellite (38) and (39). The lightning flashes were identified by the exponential decay of the signal after each flash. The lightning was associated with large systems of thunderstorms. In 1969, these results were confirmed by OSO-5.

The first Vela satellites, launched in the early 1960s, included instruments designed primarily to detect the optical radiation of the "fire ball" produced by nuclear explosions in the atmosphere. The "fire ball" also, as is well known, contained within it many lightning flashes. Special optical instruments, designed by Sandia Laboratories (40), were installed in four Vela satellites which were launched into space in the early seventies. They were positioned in an inclined circular orbit with a geocentric radius of 1.1×10^5 km. The electronic circuitry was such as to record the time history of optical signals near the earth. The power threshold of the optical energy was 10^{12} watts.

Notwithstanding the high detection threshold, the Vela satellite recorded many signals that had the characteristics of lightning. The Vela experiments established the fact that optical energy radiated by lightning could be detected by properly designed instruments on satellites. It was recognized, as a consequence of these experiments, that it is possible to monitor and count the number of global thunderstorms by more sensitive optical instruments, both for the detection and the location. In order to conduct satellite meteorological studies, during the sixties NASA and NOAA developed visual and thermal (IR) image detection and location systems that were more sensitive and more precise, respectively. The sensitivity and the spatial resolutions were very much improved over the Vela and OSO instruments. The defense establishment incorporated many of these improvements in its

series of "Defense Meteorological Satellite Program" (DMSP) satellites (41).

Analyzing selected photographic images produced by DMSP satellites, Sizoo and Whalen (42) detected the presence of horizontal streaks along a squall line. These were interpreted by them and by Orville and Vonnegut (43) to be the radiation from lightning discharges.

The following sections will contain description and discussion on the optical systems used on OSO-2, OSO-5, DMSP-33, DMSP-2, and DMSP-3 satellites.

3.1 The OSO-2B and OSO-5 Satellites

The experiments on the OSO-2B and OSO-5 satellites were designed by Prof. E. P. Ney and his group to study dim light phenomena referred to as zodiacal light (44) and (45). OSO-2B was launched in 1964 and OSO-5 was launched in 1969.

Analyzing the experimental OSO-2B zodiacal light data, Ney and associates identified light signals that had characteristics of lightning discharges. To explore further the efficacy of his optical system to detect lightning, Ney and associates designed specific photometers which were added to the zodiacal instruments used in OSO-5.

The subsequent description and discussion of OSO-2B and OSO-5 will be limited to their application to the detection of lightning discharges.

The detection concepts used on OSO-2B and OSO-5 were similar. They consist of optical systems that periodically

scanned the earth. The optical radiation emitted from the earth and the earth's atmosphere was intercepted by a number of telescopes. The optical energy was measured by photometers which had an overall spectral response extending from approximately 2900 Å to 7000 Å.

During the nighttime viewing, the photometers detected the light emitted by lightning. The identification of lightning was determined by observing the exponential decay of the signal and also by observing that the lightning was usually associated with large cloud systems which could be seen in the reflected light of the airglow. A computer was used to scan the data from the three photometers in order to separate out all abrupt increases in signals, and to discriminate against the abrupt increases due to spurious light sources.

A description of the specifics of the optical systems is given in the subsequent paragraphs.

The OSO-2B satellite was launched into a near circular orbit at an altitude of 600 km. It had an inclination of 33° to the earth's equator and a period of 96 minutes. It consisted of two components, a sail that was held perpendicular to the sun satellite direction and a wheel that rotated 30 RPM about an axis in the plane of the sail. (A diagram depicting the placement of all the components is shown in Fig. 19.) During the day the spin axis was rigidly maintained at $\leq 4^{\circ}$

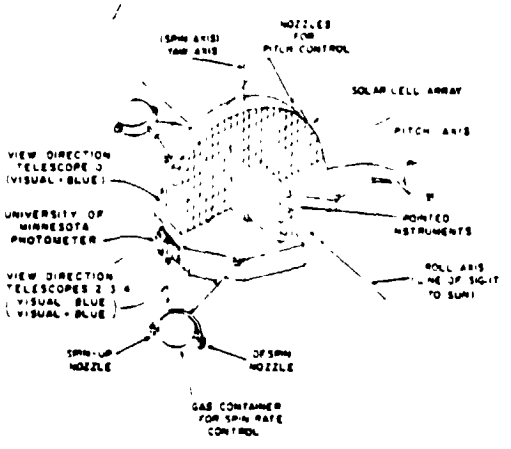

Fig. 19

Configuration of the Satellites OSO-B2, OSO-5

Source: J. G. Sparrow et al
Reference: (38)

of the plane perpendicular to the satellite sun line. At night the sail was free to rotate with the wheel.

During the night, the sail and antisail telescopes viewed the earth. Telescopes 0 and 3 (Fig. 19) were turned off during the day and turned on during the night. During the nighttime viewing, lightning discharges were observed.

The photometers viewed through fixed Polaroid sheets whose orientation with respect to the sky was governed by the rotation of the wheel. The spectral response of the various photometers is shown in Fig. 20.

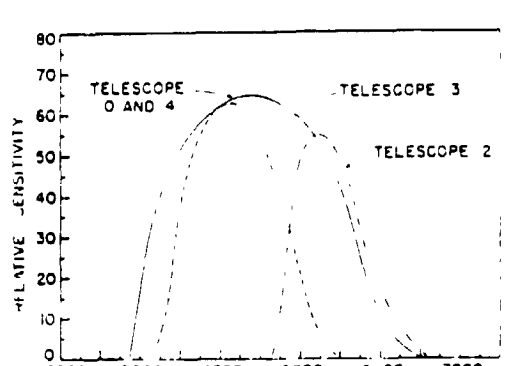

Fig. 20

Spectral Response Curves
of the Photometers
OSO-B2 and OSO-5

Source: J. G. Sparrow, et al
Reference: (38)

Three of the photometers were pointed downward toward the earth. One photometer was pointed upward along the spin axis and one was used for calibration. The photometers operated successfully from February to November, 1965, for a total of 4120 - 15 = 4105 orbits.

The instrumentation used on OSO-5 was an improved version of that used on OSO-2B. The optics and electronics associated with a number of the photometers were designed to detect more efficiently optical pulses produced by lightning discharges. Four of the photometers were capable of detecting lightning strokes. Two of the photometers were pointed in the anti-sail direction through the bottom of the spacecraft. One had a 4000 Å filter and a Polaroid filter, whereas the other had a Corning (type 2-63) 5900 Å filter. They measured the radiation from the lightning flashes extending from the blue to the far red.

As the spacecraft rotated, the instrument covered a 30^{o} cone above and below the spacecraft along the spin axis.

The calibration of the photometers was accomplished by having a known constant light source in the optical system of the photometers.

Each photometer had a 10^{o} angular diameter field of view, looking along the spin axis of the satellite in the direction opposite to that of the solar sail. The field of view of the photometers on the earth ranges from approximately $1^{o} \times 1^{o}$ when the photometers view vertically to a maximum of 12 square degrees just before the field of view leaves the earth.

OSO-2B detected about 200 storms (400 strokes). Vorpahl et al (44) computed that the number of storms during the night is of the order of 3200 which is considerably lower than Brooks' figure of 44,000 per day (1).

Sparrow and Ney (45) plotted about 1000 storm complexes from OSO-5 data. About 7,000 lightning strokes were observed during the periods February - September, 1969, (20 to 24 h. local time), and January - July, 1970, (00 to 04 h. local time). The results are similar to those acquired on OSO-2b and similar to those reported by Edgar et al (46).

The number of lightning strokes per 2 minute interval recorded in each storm complex varied from a minimum of 2 to about 30.

The photometers recorded spurious light signals that were not associated with lightning. The sources of some of these

spurious signals have been determined, whereas some sources are still unknown. Sparrow and Ney (39) concluded that sources of these spurious signals were other satellites that passed in the photometer's 10° view, cities, and burning gases of oil wells.

The lightning measurements made by OSO-2B and OSO-5 prove that the optical systems used can detect some lightning strokes and under certain conditions of visibility of the earth can associate these strokes with storm centers. The system cannot, however, define the exact area at which the lightning stroke occurs. The system does not possess the needed spatial resolution.

The authors (44), (45) have attempted to correlate the detection efficiency of their instruments with the data acquired by other observers, using different detection techniques. The correlation, by the authors' own admission, was poor. On the other hand, their global distribution of thunderstorm data agreed with other observed global data.

The results of OSO-2B and OSO-5 indicate that optical detection and noise-discrimination techniques can be used to monitor global thunderstorms during nighttime viewing of the earth's atmosphere. The attainment of more precise data on the number and geographical location of thunderstorms - viewed only at nighttimes - requires additional sophistication of the instruments.

3.2 Defense Meteorological Satellite Program (DMSP)

The sensors on board DMSP were designed to provide responsive meteorological data to the United States Air Weather Service. Specifically, the missions for DMSP (47) were to:

1. "Provide globally recorded visual and infrared cloud cover and other specialized environmental data,"
2. "Provide real time direct readout of local area environmental data", and
3. "Continue the advancement of environmental satellite technology."

The global DMSP data were and are being processed by the United States Air Force Global Weather Service. They are in archives at the University of Wisconsin and are available to all users at the National Oceanic and Atmospheric Administration (NOAA).

Many DMSP satellites were launched into orbits. This report will restrict its discussions to the DMSP satellites shown in Table 1. These particular satellites, namely DMSP-33, DMSP-2, and DMSP-3, provided extensive data on the global thunderstorm activity, and their instruments and data were discussed in the scientific journals.

The detection and the geographical spatial location techniques of terrestrial lightning flashes consisted of two scanning optical radiometers which responded to the spectral radiation within the band from 4000 - 12,000 Å. During each

scan the radiometers viewed a fixed area on earth. The input radiant energy to the optical system of the radiometers was converted into electrical signals and also into photographic images. The rate of the rise and decay times of the electrical signal were used to discriminate the lightning pulse from the d.c. electrical pulses and other noise signals. On the photographic images, the lightning flashes appear as short streaks. The geographical area from whence the flashes originated can be determined from the photographic image. The exact space coordinates of the orbiting satellite and size of geographical area that is viewed by the optical telescopes of the radiometer can be determined. Neither radiometer will offer precise locations.

The DMSP scanning radiometer optical components are shown in Fig. 21 (47). One radiometer consists of a two-channel scanner for high resolution (HR) and mode infrared (MI) data; the other scanner is a two-channel for very high resolution (VHR) data. Each radiometer consists of a mirror mounted on a shaft which rotates as the mirrors scan from the horizon to the horizon. The VHR/WHR revolves at 5.34 c/s, whereas the HR/MI revolves at 1.78 c/s. The field of view from VHR/WHR is 0.766 milliradians. The spatial resolution from an altitude of 833 km is, at the sub point, 0.61 km. The HR/MI field of view is 4.56 milliradians and the resolution at the sub point is 3.7 km. The MI detector has a 5.3 milliradian field of view and yields a resolution of 4.44 km for infrared data.

ORIGINAL PAGE IS
OF POOR QUALITY

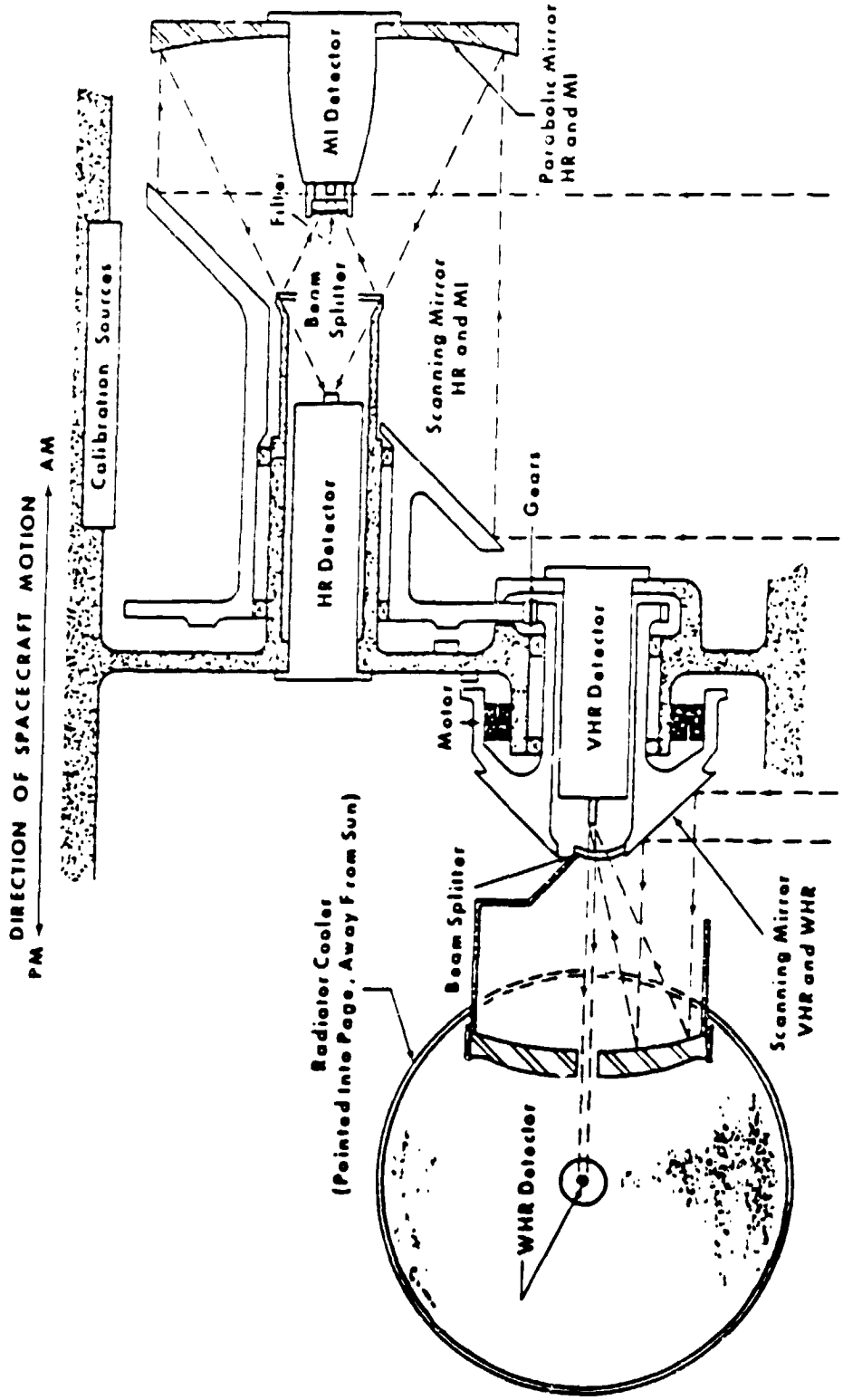

Fig. 21
DMSP Scanning Radiometer Optics

Source: United States Air Force -- W. S. Report 74-250, 1974
Reference (41)

A Special Sensor Lightning (SSL) detector, built by Aerospace Corp., was launched into an 833 km altitude orbit as a subsidiary payload on DMSP-33 (48). This sensor consisted of 12 silicon photodiodes, arranged so that each photodiode sensor viewed about 500,000 km^2 of the earth while the composite of all the sensors observed a complete field of about 7×10^6 km^2 below the satellite. The area scanned is shown in Fig. 22a (41). The sensitivity range of the photodiodes was 10^8 to 2×10^{10} watts. The minimum detectable signal was 1.5×10^{-9} watts/cm^2 and the saturation level was 2×10^{-7} watts/cm^2. Reflected sunlight saturated the sensor. The measurements were restricted to midnight times. Consequently, only a small amount of data was processed from this flight (49).

A more sensitive lightning detection system was designed and built by Sandia. It was labeled PBE-2 (Piggy Back Experiment) and was installed on DMSP-2 satellite. The instrumentation consisted of a single photodiode, amplifier, and digitizer channel. The field of view of this photodiode was a cone of 40^o half angle pointed directly downward toward the earth. It covered an area of 10^6 km^2. Fig. 22b (41) shows the single element view of the PBE-2. The detection sensitivity of PBE-2 was 4×10^9 to 10^{13} watts.

The primary purpose of PBE-2 was to extend the observation of lightning to daylight as well as darkness. To provide detection capability during daylight, sensor data electronic processing was developed to reduce the value of

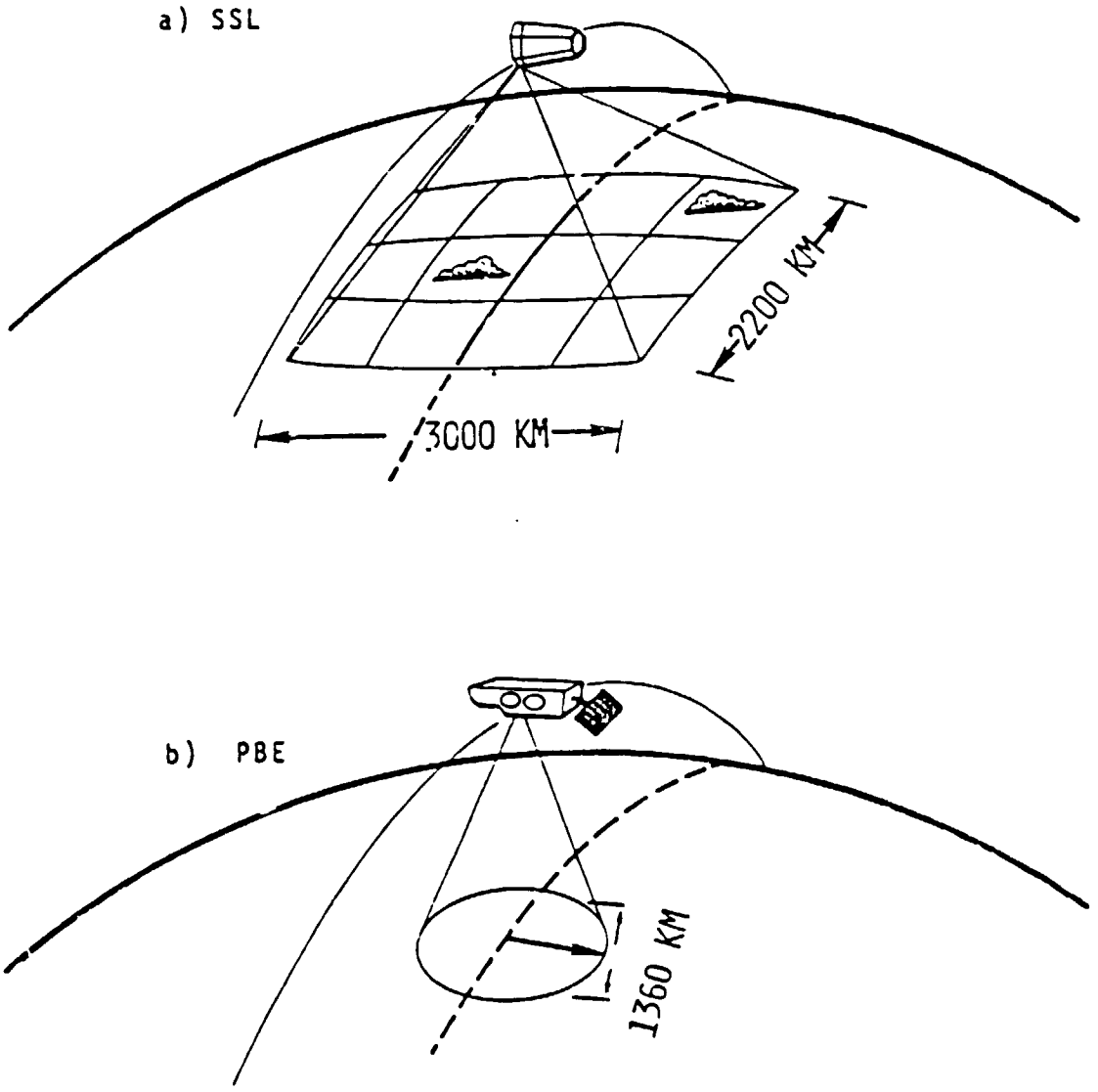

Fig. 22

Field of View of SSL and PBE Experiments
on DMSP Satellites

Source: Refernce : (41)

the d.c. component produced by the earth albedo. The electronic control was such that whenever the amplitude of the lightning signals exceeded a value of 5×10^{-8} watts/cm^2 digital sample began. The sampling rate was 31.2 KHz, giving a resolution of 32 microseconds.

False triggers, produced when the background illumination changes suddenly, are easily recognized and, therefore, eliminated from the data base.

In the DMSP-3 satellites, the lightning detection instrumentation was an improved version of PBE-2. This satellite was launched in April, 1980. To date, there is no information on the operational data in the open literature.

The DMSP satellites were launched into circular sun-synchronous orbits at an altitude of 833 km, with an inclination angle to the equatorial plane of 98.7°. The inclination angle of 98.7° was selected to insure that the 833 km circular orbit is sun-synchronous; that is, the orbital plane of the DMSP satellite rotates slowly around the earth at the same rate and direction that the earth rotates around the sun (47).

The 98.7° inclination specifies the sub-point latitude limits for the spacecraft. The spacecraft sub-point reaches 81.3° N and 81.3° S latitudes during each orbit. The sensor scans 13.3° of latitude each side of the sub-track; therefore, at each 81.3° N or S, the imagery extends past the poles.

The nodal period of this sun-synchronous orbit is 101.56 minutes.

The nodal period of 101.56 minutes indicates that the satellite will orbit 14 times per day. Furthermore, each nodal crossing will be 25.4° west of the previous crossing. Since the scanning covers 13.3 degrees (latitude and longitude) about sub-nodal point, the imagery data are contiguous about the equator.

It was mentioned that experimental data acquired by the DMSP series of satellites were in the form of photographic images as well as amplitude voltages of the received signals. Analyzing the photographic images of the DMSP satellites, Sizoo and Whalen (42) have identified the horizontal streaks in the photographs as caused by lightning. These are shown in Figs. 23 and 24 (50). In Fig. 23 the lightning flashes appear as short bursts of white lines. This infrared photograph was taken during the night without any moonlight. The radiometers on board the DMSP detected the lightning but the geographical location could not be determined because the surface of the earth was not visible. In Fig. 24 is a night visual photograph of lightning associated with an intense cold front. In this case, a full moon illuminated the surface. The lightning flashes appear as white streaks all along the front extending along the Ohio Valley. The sensor scans from left to right.

It is clear from these photographs that regional spatial ground location of lightning by these instruments is only possible if the night is illuminated fully by moonlight.

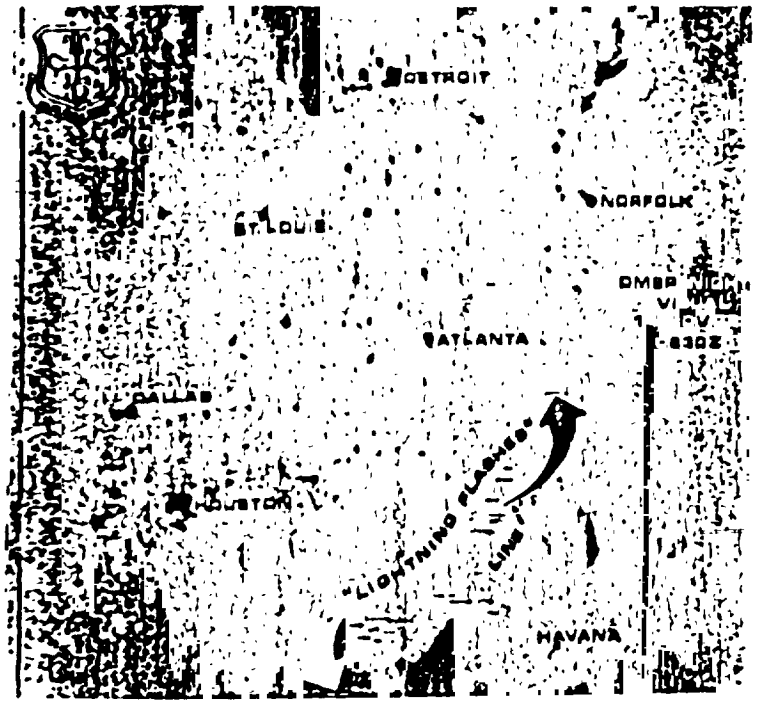

Fig. 23

DMSP Nighttime Visual Photograph of Lightning Flashes (14 Nov. 72)

Fig. 24

DMSP Nighttime Visual Photograph Depicting Lightning Flashes in an Intense Cold Front (3 Apr 74)

Source: H. W. Brandli
Reference: United States Air Force - TR - 76 - 264, August, 1976 (50)

Orville and Vonnegut (43) analyzing these same images of Fig. 23 deduced a flash frequency of 2.4×10^{-5} flashes/sec. km^2. For the storm depicted by image shown in Fig. 24, the flash frequency was 1.5×10^{-4} flashes/sec. km^2. They offered the suggestion that flash frequency of lightning could be indicative of the characteristics of different types of storms.

Orville (51) has, also, analyzed the DMSP photographs collected during September, October, and November, 1977. Figs. 25a, b, c are plots of global occurrence of lightning. Each plot shows the location of approximately 2000 flashes with respect to the major land areas. As to be expected, the concentration of storms centers around 25^{o} N to 25^{o} S latitudes. The maps reveal the paucity of storms over the water. From these data the land-ocean lightning flash frequency was computed as a function of month. These data are shown in Table 11.

TABLE 11

Ratio of Land-Ocean Flash Frequency

Month	Month Flashes Recorded	Land-Ocean Ratio
September	1813	1.58
October	2121	1.53
November	2178	1.95

The land-ocean ratios reported differ by a value of 10 from those that were reported by Vorphal (44), and by a value of 8 that were reported by Orville and Spencer (52). Orville stated

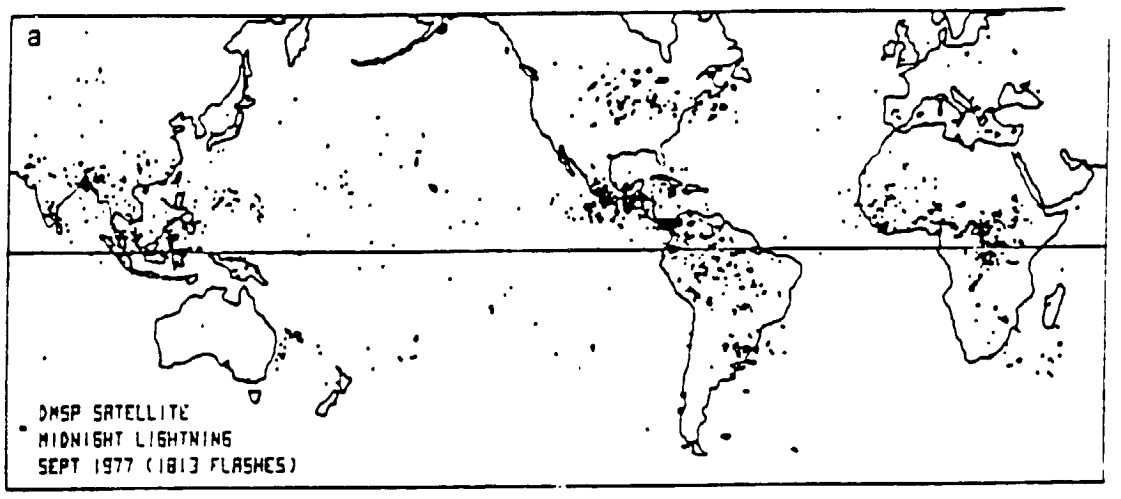

Midnight lightning positions recorded by the DMSP satellite for the month of September 1977.

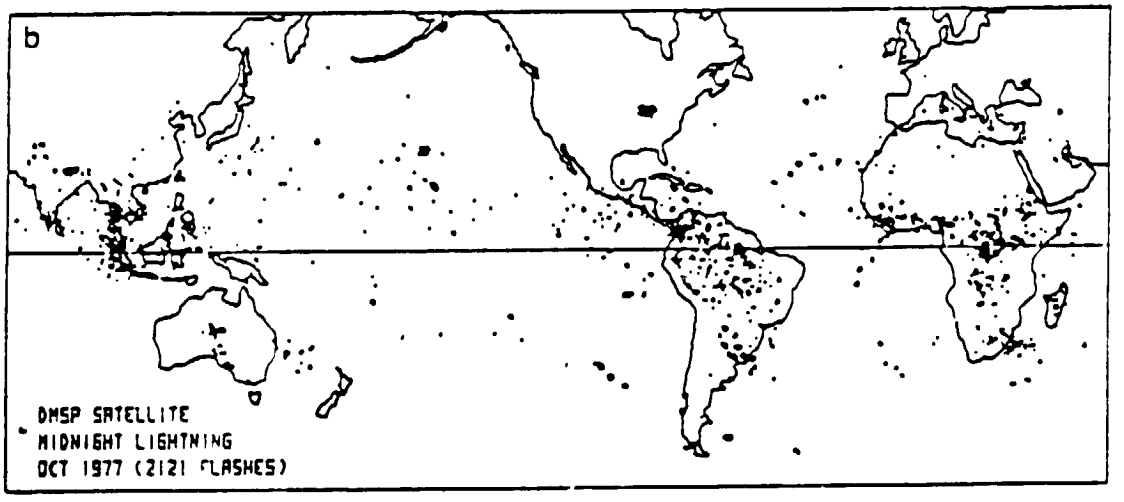

Midnight lightning positions recorded by DMSP satellite for the month of October 1977.

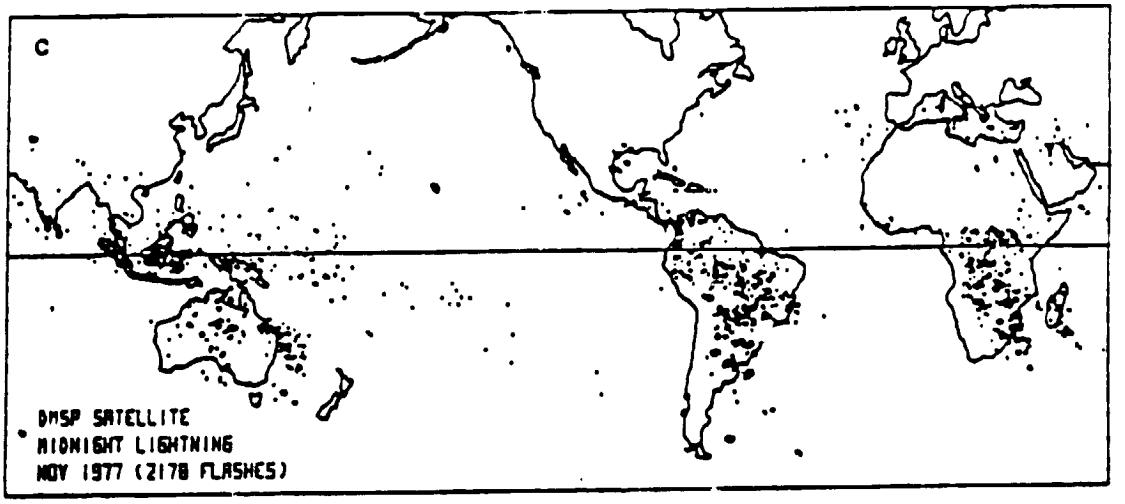

Midnight lightning positions recorded by the DMSP satellite for the month of November 1977.

Fig. 25

Source: R. Orville
Reference: (51)

that the large discrepancy of 10 was due to the classification of ocean flashes that occurred within 300 - 400 km from the coast as land flashes. Reducing the extent of classification to 50 km from the coast reduces the error to 4.

Croft (53) has noted that over the south Atlantic unusual lightning streaks were recorded in DMSP photographs. He concluded that these were due to the satellite penetrating through the Van Allen Belt. The streaks thus generated were much longer than those due to thunderstorm lightning.

The radiometric data acquired by the DMSP-33 satellite with the SSL (Special Sensor Lightning) sensor and by DMSP flight 2 with the PBE-2 lightning sensor have been analyzed and reported primarily by Turman (40) and (49), by Edgar et al (46), and by Turman and Edgar (54), (55).

The DMSP-SSL used the scanning scheme shown in Fig. 22a to accumulate its data. Each point on the earth's surface within 1500 km of the satellite subtrack was viewed consecutively by the three photodiodes for a total period in excess of 5 minutes. The nominal range for the central photodiodes was 920 km and for those on the edge, it was 1600 km.

The data were acquired for 15 orbits during the period from September, 1974, to March, 1975. Thunderstorms were observed during ten of the orbits and approximately 10,000 were recorded from 24 storm complexes. Notwithstanding, a limited amount of data was processed.

From these data Turman (49) derived a cumulative frequency distribution of power using a total of 4652 lightning flashes. He found that the source median power level was 1×10^9 watts and that 98% of the flashes had peak power less than 1×10^{10} watts. The peak power varied from 10 to 2000×10^8 watts. The distribution is shown in Table 12.

TABLE 12

Frequency Distribution of Peak Optical Power from SSL Data (Source: Turman, Ref. 49)

Power Range 10^8 W	Number	Normalized Fraction	Cumulative Fraction
1 - 2	387	0.083	0.083
2 - 5	932	0.200	0.283
5 - 10	895	0.193	0.475
10 - 20	935	0.210	0.676
20 - 50	1106	0.238	0.914
50 - 100	318	0.068	0.982
100 - 200	66	0.014	0.996
200	13	0.003	1.00

Turman (49) derived from these SSL data the average flash rate per unit surface area as 5×10^{-6} to 2×10^{-4} s^{-1} km^{-2}. The surface area considered is that area which is under the view of the sensor. He concluded that the count rate correlated well with the occurrence of cumulo-nimbus and related cloud formation.

The DMSP flights 2 and 3 have recorded approximately 30,000 lightning triggers. Not all of these data have been analyzed. Analyzing some of the accumulated data, Turman and Edgar (54) report that 90% of the PBE pulses had rise times

of = 0.2 milliseconds and 80% had pulse duration of = 0.7 milliseconds. A representative sample of the rise and decays as well as the wave shapes of the pulse are shown in Fig. 26. 80 to 90% of the observed lightning flashes had the wave forms shown in Fig. 26a. About 10 to 20% had a wave form shown in Figs. 26b and 26c.

Turman (40) computed the lightning count rate for each geographical region. The computation was performed by counting the number of lightning strokes detected while the satellite sub-point was within that region and by dividing by the total time the sub-point was within that region. In Table 13 Turman (40) summarized the total lightning counts and the integrated count rate for August - November, 1977.

TABLE 13

Total Counts
and Integrated Count Rate of Lightning

Period 1977	Dawn		Dusk	
	Total	Per Minute	Total	Per Minute
Aug. - Sept.	2460	0.2	3013	0.3
Sept. - Oct.	3871	0.3	2700	0.2
Nov.	2605	0.2	1269	0.1

The optical detection threshold of the DMSP-2 and -3 was 5×10^{9} watts; hence, only a very small fraction of the global thunderstorm activity was recorded. Comparing the results achieved in the DMSP-PBE experiment with those reported by others in the literature, Turman and Edgar (54) (55) concluded that the DMSP-PBE detected only 2% of all the lightning flashes within its field of view.

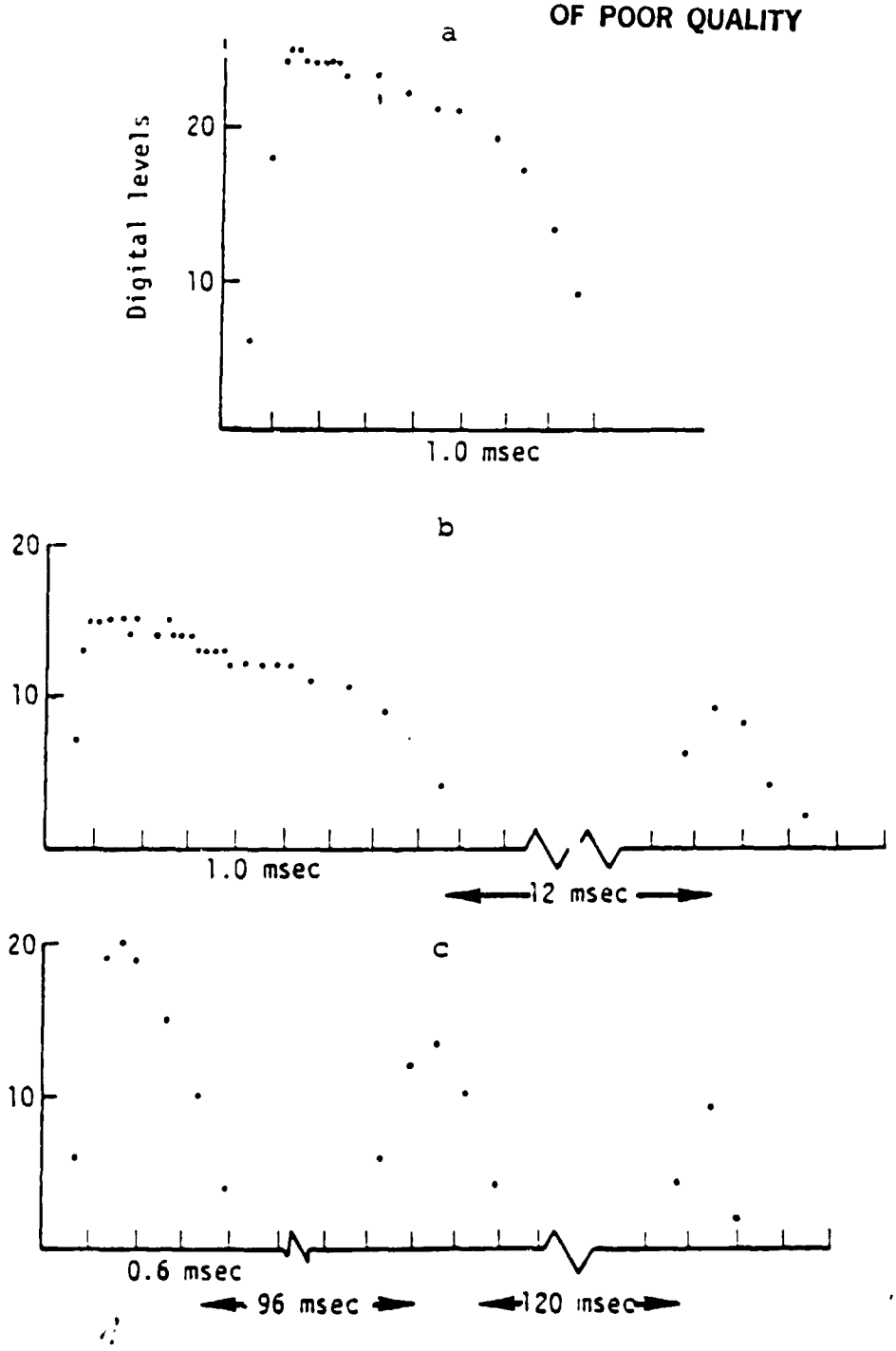

Fig. 26

Representative PBE Lightning Wave Forms. Timing Resolution is 32 Microseconds; Some Data Points Are Omitted for Clarity. (DMSP - PBE Sattelite)

Source: B. N. Turman and B. C. Edgar
Reference: (54)

In summary, the meticulous analysis of the lightning streaks on the DMSP infrared photographic images does yield information on thunderstorm activity over extensive geographical regions. The geographical regions were determined only when there was sufficient moonlight illumination to make the earth's surface visible. This scheme, if applied to the analysis of all the infrared images recorded by the DMSP satellites, will yield, on sound statistical basis, a more accurate global distribution of thunderstorm activity than is available today. It will also provide a more accurate count of the number of lightning flashes.

The derived global distribution of thunderstorm activities is in agreement, in a general way, with other distribution recorded by other investigations.

The detection threshold of the optical system was too high. Its value was approximately 10^9 watts. As a consequence, many of the lightning flashes were not detected by this series of satellites. DMSP did, however, record 30,000 lightning flashes. Even so, the system detected only 2% of all the lightning flashes that occurred within the view of its optical telescope. This fact represents a very low detection efficiency.

IV Summary of Source Characteristics and Satellite Results

1. General Remarks

A review of the literature revealed that the satellites listed in Table 1 detected and measured electrical and optical signals produced by terrestrial thunderstorms.

Lofti-1 detected and measured the VLF (18KHz) signals when the satellite was overhead the thunderstorm. Alouette and Ariel II and RAE-1 recorded lightning pulse in the frequency band of 0.4 to 11.5 MHz. OSO-2B and Vela-B recorded optical signals, the sources of which were identified to be terrestrial lightning.

Ariel III, OSO-5, DMSP, and ISS-b satellites detected and measured the magnitude of a number of parameters related to lightning. The parameters that these satellites measured or attempted to measure were the electrical and optical energy, the time histories and the wave forms of the energy pulses, the number of pulses per unit time, and the determination of the geographical sources of the pulses. To evaluate the effectiveness of the systems used in these satellites, it is necessary to know the characteristics and the magnitudes of these parameters at the source, that is, the thunderstorm complex.

2. Source Characteristics

Shown in Table 8 are the experimentally determined values of the source parameters that are relevant to the design of satellite systems in order to monitor thunderstorms. These parameters were determined by measurements made on the surface of the earth. It is evident that the peak power of lightning flash varies from 10^7 to 10^{12} watts. Krider (21) measured the electrical and optical peak power of a lightning flash to be 1.4×10^{12} and 1.1×10^{10} watts, respectively. Turman (22) found the radiated optical power to vary from 2×10^9 to 2×10^{11} watts. Using optical experimental data acquired 20 km above and 20 km distant from a thundercloud, Brook

et al (23) calculated the peak power of lightning flashes and found the power to vary in value from 10^8 to 10^{10} watts.

The electrical field as measured at a distance of 10 km from the source is found to vary from a value of 10^6 μV/m at .01 MHz to 10^2 μV/m at 100 MHz. These values represent the computed average values of the experimental data acquired by many investigators.

Barasch (24) made a number of ground measurements of power of specific spectral lines radiated from a single stroke. The relative intensities of the spectral lines, as seen in Table 8, varied from 1 at 3914 Å to 4.8 at 8220 Å. The most probable value of 3914 Å line is about 4×10^4 Wsr^{-1} A^{-1}. Brook (14) found that the average value of the ratio of the irradiance of the 6563 Å to 3914 Å for all lightning pulses to be 5.6.

The average rise time of an optical pulse, produced by a return stroke, is approximately 100 μs and the decay time is about 300 to 1000 μs. The time histories of the various optical pulses are governed by the type of lightning discharge occurring in the thundercloud.

3. Satellite Results

Lofti-1

The Lofti-1 experiments proved that the 18 KHz signal does penetrate the ionosphere, and, therefore, is detectable and measurable within and above the ionosphere. During a dawn pass at a height of 400 km over Central America and during the daylight part of the pass, several noise peaks due to

lightning had values between 10 μV/m and 100 μV/m. The propagation losses through the ionosphere during daylight hours were computed to be approximately 38 dB and 13 dB during night hours.

Alouette

r.f. tuned receivers covering the band (0.4 to 11.5 MHz) detected r.f. pulses produced by terrestrial lightning.

Ariel III

The Ariel III detected and located terrestrial lightning flashes. It used two narrow band receivers, one tuned to 10 MHz and the other tuned to 15 MHz. The maximum recorded field strength was 1.6×10^{-3} V/m. The area of the ground viewed by Ariel III at the time was 8.3×10^{5} km^2.

ISS-b

Tuned r.f. (5 - 25 MHz) circuits were used to detect lightning pulse, and also to discriminate against extraneous noise signals. The ionospheric "IRIS" effect was used to locate geographical source of lightning. The ISS-b accumulated reams of data on lightning discharges.

Kotaki et al (34) calculated the lightning frequency per unit area to be 1.2×10^{-5} sec^{-1} km^{-2}, the global frequency of lightning discharge to be 63 sec^{-1}, and the peak power flux of a lightning pulse to be 1.4×10^{-13} wm^{-2} (KHz)$^{-1}$.

During part of one orbit the ISS-b lightning data were compared with the number of thunderstorms recorded by the Geostationary Meterological Satellite. The correlation between these two sets of data was poor. Thirty to fifty percent of the data had been affected by the high level of noise

signals. Global maps of thunderstorm activity were derived from the data.

The area viewed by the satellite was $.8 \times 10^{-6}$ km^2.

Vela-B

The lightning flash signals were detected by tuned r.f. circuits. The data indicate that lightning flashes were poorly identified, and the location of the sources could not be accurately determined. The correlation of Vela-B data with meteorological ground data and with the occurrence and location of thundery regions was extremely poor.

RAE-1

The concept of detecting and determining the source of lightning flashes was similar to one used by Ariel III. It measured noise signals, including lightning pulse, at an altitude of approximately 6000 km. The analysis of the data provided contour maps of global terrestrial radio noise distribution. It did not provide quality nor quantity data on the number or the location of terrestrial lightning.

OSO-2B and OSO-5

OSO-2B and OSO-5 used similar optical detection systems that periodically scanned the earth. The optical radiation (2900 - 7000 Å) emitted from the earth and from the earth's atmosphere was intercepted by a number of photometers. The photometers detected lightning only during nighttime. The lightning was identified as rapid increases in the value of signal intensity, followed by its exponential decrease to background values.

OSO-2B detected about 400 lightning strokes and OSO-5 detected about 7000 strokes. From these data seasonal maps of thunderstorm activity were derived.

The number of lightning strokes per two minute intervals recorded in each thunderstorm complex varied from a minimum of 2 to about 30.

The system lacked the capability to define the exact area at which lightning strokes occur.

DMSP

On the DMSP satellites, the detection and the geographical spatial location techniques of terrestrial lightning flashes consisted of two scanning optical radiometers which responded to the spectral radiation within the band 4000 - 12,000 Å. During each scan the radiometers viewed a fixed area on the earth. The input radiant energy to the optical system of the radiometers was converted into electrical signals and also into photographic images. The rate of the rise and decay times of the electrical and optical signals was used to discriminate the lightning pulse from the d.c. electrical pulses and other noise signals.

The DMSP-SSL optical system consisted of 12 silicon photodiodes arranged so that each photodiode viewed about 500,000 km^2 of the earth while the composite of all sensors observed a complete field of 7×10^6 km^2 below the satellite. The sensitivity range in units of input power to the lightning channel of the diodes was 10^8 - 10^{10} watts.

The DMSP-PBE-2 consisted of a single photodiode. Its

field of view covered an area of 10^6 km^2. Its detection sensitivity ranged from 5 x 10^9 to 10^{13} watts.

Orville and Vonnegut (43) analyzing the photographic images deduced flash frequencies of 1.5 x 10^{-4} to 2.4 x 10^{-5} flashes/sec. km^2. Orville (51) found the ratio of land to ocean flash frequency to be 1.68. Global contour maps of lightning detected at midnight were prepared.

Turman (40) derived accumulative frequency distribution of power of lightning flashes. The peak power varied from 10^9 to 2 x 10^{11} watts; the median was 10^9 watts. 98% of the flashes had peak power less than 1 x 10^{10} watts. The flash rate on the surface varied from 5 x 10^{-6} to 2 x 10^{-4} sec^{-1} km^{-2}.

The DMSP-PBE-2 and -3 satellites recorded approximately 30,000 lightning strokes. Not all of these have been analyzed. Comparing the results achieved by the DMSP-PBE satellite with other ground meteorological data, Turman and Edgar (54) found that DMSP-PBE detected only about 2% of all the lightning flashes within its field of view. From the DMSP-PBE-2 data wave shapes of the optical pulses were derived. 90% of the pulses had rise times of 0.2 milliseconds and 80% had pulse duration of 0.7 milliseconds.

The operational specifications of those satellites that were instrumented to study the characteristics of lightning are shown in Table 14. In the first column, the satellites are listed in order of their achievements. The total field of view of the detection system is given. The geographical spatial resolution is given in column three.

TABLE 14

Operational "Specs" of Satellites

Satellite	Total Area Viewed $\times 10^6$ km^2	Spatial Resolution $\times 10^6$ km^2	Sensitivity: Input to System	Power Input to Lightning Flash $\times 10^9$ watts
DMSP - PBE	1	1	$10^{-8} - 10^{-10}$ w/m^2	$5 - 10^4$
DMSP - SSL	7	0.5	$10^{-9} - 10^{-7}$ w/m^2	$1 - 10^2$
ISS-b	0.8	0.8	$10^{-15} - 10^{-13}$ wm^{-2} (KHz)$^{-1}$	-
Ariel III	0.8	0.8	$1 - 10^3$ μV/m	-
OSO - 5	0.14	0.14	3×10^5 photon/cm^2	-

The sensitivity of the system is expressed in two different units, one as the value of the input signal, and, the other as power radiated by the lightning stroke at the source. A range of values is given. It is to be noted that units differ for each satellite. These were the units expressed by the authors of the various papers that were reviewed.

4. Rating of Satellites

The performance and rating of each satellite are presented and assessed in Table 15 in terms of topics related to global thunderstorm activities as defined in Table 2. The judgement expressed as "yes" and "no" in Table 15 was predicated on the answer to two questions. First, does the satellite satisfy, partially or wholly, the requirements set forth in Table 2? Second, can explicit information be derived from the experimental data to satisfy those requirements?

The DMSP-SSL and DMSP-PBE, from a technical point of view, used a system that provided photometric data and photographic images of lightning flashes. These satellites provided the most precise data on the thunderstorms even though their data gathering efficiency was low.

The ISS-b and the Ariel III satellites were moderately effective in detecting powerful lightning flashes. They failed to detect and record the less powerful flashes because they were submerged in the noise. The r.f. technique used to discriminate against the undesired noise signals was too effective. Furthermore, the geographical spatial resolution of these satellites was poor.

TABLE 15

Performance and Rating of Satellites

		Thunderstorms					Lightning Discharges							
Rating	Satellite	Global Distribution	Regional Distribution	Exact Location	Seasonal Occurrence	Correlation with Ground - Net. Data	Exact Count	Frequency per Unit Area	Global Frequency	Time History of Pulse	Power/Pulse	Percent of Pulses Detected in F.O.V.	Real Time Information
1	DMSP - PBE	Yes	Yes	No	Yes	Poor	No	Yes	Yes	Yes	Yes	2	No
2	*DMSP - SSL	No	No	No	No	Poor	No	Yes	Yes	Yes	Yes	90	N
3	ISS-b	Yes	Yes	No	Yes	Poor	No	Yes	Yes	No	Yes	30	No
4	Ariel III	Yes	Yes	No	Yes	Poor	No	Yes	Yes	No	Yes	--	No
5	*OSO-2 - OSO-5	No	No	No	No	Poor	No	No	No	No	No	--	No
6	RAE-1	Yes	Yes	No	No	Poor	No	No	No	No	No	--	No
7	Vela B	No	No	No	No	----	No	No	No	No	No	--	No
8	Lofti-1	No	No	No	No	----	No	No	No	No	No	--	No
9	Alouette	No	No	No	No	----	No	No	No	No	No	--	No

* Nighttime observations only

F.O.V. = Field of View

The optical detection system of the OSO-5 was very sensitive. However, it could only operate during the night. Its geographical spatial resolution was also poor.

Unlike the DMSP, ISS-b, and OSO-5, the other satellites listed in Table 15 were not specifically instrumented to detect lightning flashes. They were more concerned with their particular scientific and engineering missions. The detection of lightng flashes was incidental.

V Discussion and Recommendations

The experimental data and results acquired by the orbiting satellites that were discussed in this review indicate that the scientific and technical objectives, such as precise information on the intensity, the number, and the location of lightning flashes as well as the adequate knowledge on the characteristics of lightning phenomenon, cannot be attained. The instruments used in these satellites did not have the sensitivity to detect the lightning pulse whose source had power values less than 10^8 watts, did not have the spatial resolution to define the geographical sources of lightning to an accuracy of 25 km^2, and did not have the capability to discriminate definitively the lightning pulse from other noise signals. It is evident that improved techniques and instruments are needed and must be developed and applied.

The development of improved satellite detection systems requires the availability of more precise data of the lightning

parameters as measured above the thundercloud. The critical data needed are:

1. The absolute value of the electrical and optical emissions from the first and subsequent lightning strokes,
2. The frequency (10 KHz to 50 MHz) spectrum of the electrical emission,
3. The intensity of the spectral (3000 - 12,000 Å) emission lines,
4. The wave form and the time history of the optical pulses, and
5. The ratio of the number of electrical to the number of optical pulses.

Item 1 will define the sensitivity required by the satellite instruments to detect all of the lightning strokes. Items 2, 3, and 4 will provide technical data that could be valuable in developing discrimination concepts. Item 5 can serve as a "yardstick" to evaluate the effectiveness of any hybrid electrical-optical detection system used in the satellite.

It is strongly recommended that the proposed measurements above the cloud be seriously considered, as well as the simultaneous measurements below the cloud.

Vonnegut et al (56) and Christian (57) have plans to measure some of these quantities above and below thunderstorms.

A perusal of the satellite data leads one to jump to the hasty conclusion that a system of three or more appropriately

placed orbiting geosynchronous satellites could fulfill the scientific and technical objectives that are defined in Table 2. Coroniti (58) and Massa and Coroniti (59) have proposed such a system. It is not obvious that a geosynchronous satellite will, indeed, provide the needed information. At 1000 km altitude, the present instruments in the satellites reviewed in this report had sensitivities to detect the equivalent of 10^8 watts of optical and electrical energy radiated by lightning flash. The detection efficiency was very poor. At geosynchronous altitude of approximately 36×10^3 km the intensity of all terrestrial signals will decrease by an additional factor of approximately 10^3. The sensitivity of the detection instruments in the geosynchronous satellites, therefore, must be increased by at least - if not more than - a factor of 10^3.

The same rationale can be applied to the geographical spatial resolution problem.

The data banks of NASA and NOAA have many meteorological photographs of the terrestrial atmosphere acquired by the geostationary satellites. It is recommended that pertinent data from these archives should be critically analyzed to determine:

1. Whether lightning discharges have been detected,
2. The intensity of the incident optical energy,
3. The geographical spatial resolution of the particular optical system used, and

4. The efficiency of detection by comparing the satellite data with ground based data.

The result of the analysis should be conducive to a definition of the detection sensitivity and the geographical spatial resolution required to monitor regional and global thunderstorm activity from a geosynchronous satellite.

Sophisticated electrical and optical systems are presently in use in geosynchronous satellites to measure, in various forms, the electrical and optical energies emitted by the earth and by the earth's atmosphere. It is recommended that a study of these systems be initiated in order to determine their applicability - in their present or modified versions - to the problem of monitoring severe thunderstorms.

Perusal of the scientific papers and reports in this review did not indicate conclusively whether the electrical or the optical satellite system was more efficient in detecting and locating lightning flashes. This uncertainty should be resolved. It is recommended that a study to resolve this question be initiated.

This study appears to indicate that the electrical system is more sensitive in detecting the energy radiated by the first and subsequent lightning strokes; whereas, the optical system is more effective in locating geographically the source of lightning. It is recommended that a study be initiated to study the feasibility of a hybrid electrical - optical satellite system to monitor severe storms.

The location of precise positions of lightning discharges by satellite appears to be a formidable task. Many ground-based electrical systems to detect and locate lightning have been developed and are currently in operation. A hybrid system consisting of ground-based satellite equipments could provide a viable system for monitoring thunderstorm activity. The ground system could provide accurate geographical coordinate data on the source of lighting discharge as well as data on the number of discharges. It could also provide a precise "time-hack" signal. All of these data can be transmitted to the satellite where they can be correlated and processed in conjunction with the photographic satellite data.

It is recommended that the feasibility of a ground - satellite hybrid system be studied.

The Lofti-1 experiment proved that the energetic 18 KHz signal produced by lightning does penetrate the ionosphere. It measured signal strengths of 10 to 100 μV/m at 400 km. Modern communication receivers have a sensitivity of 0.1 μV/m with signal to noise ratio of 60 dB or more. Incorporation of these improved electronic circuits to VLF receivers assures the detection of all the lightning flashes. In addition, the VLF signal could be used as the basic "time" signal to integrate the satellite and the gound network data. It is recommended that:

1. A search of the technical and scientific literature be initiated in order to find out if other

investigators have measured these VLF signals in and above the ionosphere, and

2. Additional measurements of VLF signals be made above the ionosphere.

REFERENCES

(1) Brooks, C. E. P., "The Distribution of Thunderstorms over the Globe", Geophysical Memoirs, London 24, 1925.

(2) Christensen, L. S., W. Frost, W. W. Vaughn, NASA-CP-2095, Proc.: Workshop on the Need for Lightning Observation from Space, July, 1979.

(3) Uman, M. A., "Lightning", published by McGraw Hill Book Company, 1969.

(4) Schonland, B. F. J., "Atmospheric Electricity", published by John Wiley & Sons, New York, and also by Methuen & Co., Ltd., London, 1953.

(5) Israel, H., "Atmosphaerische Elektrizitat", Teil 1 and Teil 2, published by Akademishe Verlagsgesellschaft Geest & Portig K.-G., Leipzig, 1957. Note: Translations of these two volumes are available from "The U. S. Department of Commerce, National Technical Information Service, Springfield, VA 22151.

(6) Chalmers, J. Alan, "Atmospheric Electricity", published by Pergamon Press, London, 1957.

(7) Kitagawa, N., "Physics of Lightning and Sferics", p.p. 663 to 682 of Ref. 12.

(8) Holzer, R. E. and W. E. Smith, editors, "Proceedings on the Conference on Atmospheric Electricity Held in 1954", published as U. S. Air Force Geophysical Research Papers, No. 42, Bedford, Mass., 1955.

(9) Smith, L. G., editor, "Recent Advances in Atmospheric Electricity", (Proc. of Second Conference on Atmospheric Electricity, 1958), Pergamon Press, London XV, 1958.

(10) Coroniti, S. C., editor, "Problems of Atmospheric and Space Electricity", (Proc. of Third Conference on Atmospheric Electricity, 1963), published by Elsevier Publ. Co., Amsterdam XIV, 1965.

(11) Coroniti, S. C. and J. Hughes, editors, "Planetary Electrodynamics", 2 vols., (Proc. of the Fourth Conference on Atmospheric Electricity, 1968), published by Gordon-Breach, New York, 1969

(12) Dolezalek, H. and R. Reiter, editors, "Electrical Processes in Atmospheres", (Proc. of Fifth Conference on Atmospheric Electricity, 1974), published by Dr. Dietrich Steinkopff Verlag, Darmstadt, Germany, 1977.

(13) Pierce, E. T., "Atmospheric and Radio Noise", published by Stanford Research Institute, Menlo Park, CA 94205, September, 1975.

(14) Brook, M., "Lightning Properties and Associated Missions". NASA Report No. CP-2095, (See Ref. 2).

(15) Oetzel, G. N., and E. T. Pierce, "Radio Emissions from Close Lightning", p.p. 543, Vol. 1 of Ref. 10.

(16) Kimpari, A., "Electromagnetic Energy Radiated from Lightning", p.p. 353-365 of Ref. 10.

(17) Horner, F., "Radio Noise in Space Originating in Natural Sources", Planetary Science, Vol. 13, p.p. 1137 - 1150, 1965.

(18) Horner, F. and P. A. Bradley, "Spectra of Atmospherics from Nearby Lightning Discharges", J. Atmos. Terr. Physics 26, p.p. 1155 - 1164, 1964.

(19) Weidman, D. D., E. P. Krider, and M. A. Uman. "Lightning Amplitude Spectra in the Interval from 100 Kz to 20 MHz", Geophysical Research Letters, Vol. 8, No. 8, p.p. 931 - 934, August, 1981.

(20) Malan, D. J., "Radiation from Lightning Discharges and Its Relation to Discharge Process", p.p. 557 - 563 of Ref. 8.

(21) Krider, E. P., G. A. Dawson, M. A. Uman, "Peak Power and Energy Dissipation in a Single Stroke Lightning Flash", Jour. Geophy. Res. 73, p.p. 3335 - 3339, 1968.

(22) Turman, B. N., "Lightning Detection from Space", Scientific American, May - June, 1979.

(23) Brook, M, Richard Tennis, C. Rhodes, P. Krehbiel, B. Vonnegut, and O. H. Vaughn, "Simultaneous Observations of Lightning Radiations from Above and Below Clouds", Geophysical Research Letters, Vol. 7, No. 4, pp. 267 - 270, April, 1980.

(24) Barasch, G. E., "The Lightning Spectrum as Measured by Collimated Detectors, Atmospheric Transmission, Spectral Intensity Radiated", Report No. LA - 3755, Los Alamos Scientific Laboratory, University of California, Los Alamos, New Mexico, 1968.

(25) Barasch, G. E., "Spectral Intensities Emitted by Lightning Discharges", Jour. Geophy. Res., Vol. 75, No. 6, February 20, 1970.

(26) Leiphart, J. P.., R. W. Zeek, L. S. Bearce, and E. Toth, "Penetration of the Ionosphere by Very Low Frequency Radio Signals. Interim Results of Lofti-I Experiment", Proc. of the IRE, p.p. 6 - 17, January, 1962.

(27) Warren, E. S., "Some Preliminary Results of Sounding of the Top of the Atmosphere by Radio Pulses from a Satellite", Nature, p.p. 636 - 639, February 16, 1963.

(28) King, J. W., "Investigations of the Upper Ionosphere Deduced from Topside Sounder Data", Nature, February 16, 1963.

(29) Lockwood, G. E. K. and L. E. Petrie, "Low Latitude Field Aligned Ionization Observed by the Alouette Topside Sounder", Planetary Space Science, Vol. 11, pp. 327 - 330, 1963.

(30) Longille, R. C. and J. C. Scott, Jour. of British Institute of Radio Engineers, 23, No. 1, pp. 68, 1962. (Quoted in Ref. 29)

(31) Harden, B. N. and V. A. W. Harrison, Radio Electronic Eng. 35, p.p. 125 - 133, 1968. (Quoted in Ref. 35.)

(32) Horner, F. and R. B. Bent, "Measurement of Terrestrial Radio Noise", Proc. Royal Society A, 311, p.p. 527 - 542, 1969.

(33) Ladd, A. C. and J. F. Smith, "An Introduction to Ariel III Satellite Project", Proc. of Royal Soc. A, 311, p.p. 479 - 487, 1969.

(34) Kotaki, Minoru and C. Katoh, "The Global Distribution of Thunderstorm Activity Observed by the Ionosphere Sounding Satellite ISS-b", J. Radio Research Laboratory (Japan), Vol. 28, No. 125, 1981.

(35) Kotaki, M., I. Kuriki, C. Katoh, and H. Sugiuchi, "The Effects of the Ionosphere on the Extent of the Radio Horizon at High Frequency Band", J. Radio Research Laboratory (Japan), Vol. 28, No. 125, 1981.

(36) Chiburis, R. L. and R. D. Jones, "Severe Storm Observation from Vela 4B Satellite", NRL Report 7763, Proc. Waldorf Conference on Long Range Geographical Estimation of Lightning Sources, p.p. 264 - 282, July, 1974.

(37) Herman, J. R., G. A. Caruso, R. G. Stone, "Radio Astronomy Explorer (RAE-1) Observation of Terrestrial Radio Noise", NRL Report 7763, Proc. Waldorf Conference on Long Range Geographic Estimation of Lightning Sources, p.p. 283 - 331, July, 1974.

(38) Sparrow, J. G., E. P. Ney, G. B. Burnett, and J. W. Stoddart, "Air Glow Observations from CSO-B2 Satellite", Jour. of Geophys. Res. Space Physics, Vol. 73, No. 3, p.p. 857, February, 1968.

(39) Sparrow, J. G. and E. P. Ney, "Discrete Light Sources Observed by Satellites", Science, Vol. 161, p.p. 459 - 460, August 12, 1968.

(40) Turman, B. N., "A Review of Satellite Experiments", NASA-CP-2095, "Proc. Workshop on the Need for Lightning Observations from Space", Editors: L. S. Christensen, W. Frost, W. W. Vaughn, 1979.

(41) United States Air Force Report AWS-TR-74250, 1974.

(42) Sizoo, A. H. and J. A. Whalen, Jour. of Applied Meteorology, 1976.

(43) Orville, R. E. and B. Vonnegut, "Lightning Detection from Satellite", Proc. of Fifth International Conference on Atmospheric Electricity, Editors: H. Dolezalek and R. Reiter, published by Steinkopff Verlag, Darmstadt, Germany, 1977.

(44) Vorpahl, J. A., J. G. Sparrow, and E. P. Ney, "Satellite Observation of Lightning", Science, Vol. 169, p.p. 860 - 862, August 28, 1970.

(45) Sparrow, J. G. and E. P. Ney, "Lightning Observation by Satellite", Nature, Vol. 232, No. 5312, p.p. 540 - 541, August 20, 1971.

(46) Edgar, B. C., L. M. Friese, B. N. Turman, W. H. Beasely, M. A. Uman, Y. Lin, G. F. Jacobs, and D. C. Beck, "Satellite Optical Sensing of Lightning Activity over Eastern United States and Gulf Region", Report No. SSL 79 (4639), Aerospace Corp., Los Angeles, CA.

(47) Defense Meteorological Satellite Program (DMSP) - User's Guide, Report No. AWS-TR-74-250, United States Air Force Air Weather Service, 1 December, 1974.

(48) Turman, B. N., "Lightning Detection from Space", American Scientist, May - June, 1979.

(49) Turman, B. N., "Analysis of Lightning Data from DMSP Satellite", Jour. Geophys. Res. 83, p.p. 5019, 1978.

(50) Brandli, H. W. "Satellite Meteorology", United States Air Force Air Weather Service, AWS-TR-76-264, August, 1976.

(51) Orville, R., "Global Distribution of Midnight Lightning - September - November, 1977", Monthly Weather Review, Vol. 109, p.p. 391 - 395, February, 1981.

(52) Orville, R. and D. W. Spenser, "Global Lightning Flash Frequency", Monthly Weather Review, Vol. 107, p.p. 934 - 943, 1979.

(53) Croft, T. A., "Nocturnal Images of the Earth from Space", Stanford Research Institute Report No. 68179.

(54) Turman, B. N. and B. C. Edgar, "Global Lightning Distribution at Dawn and Dusk", Report published by Department of Physics of the United States Air Force Academy, Colorado 80840, May, 1980.

(55) Turman, B. N. and B. C. Edgar, "Global Lightning Distribution at Dawn and Dusk", Jour. of Geophys., Vol. 87, No. C2, p.p. 1191 - 1206, February 20, 1982.

(56) Vonnegut, B., Otha H. Vaughn, Jr., and Marx Brock, "Nighttime/Daytime Optical Survey of Lightning and Convective Phenomena Experiment", NASA-TM-78261, George C. Marshall Space Flight Center, Marshall Space Flight Center, ALA., February, 1980.

(57) Christian, H. J., "Detection of Lightning from Space", Preliminary Study, Report published by NASA, Marshall Space Flight Center, April, 1981.

(58) Coroniti, S. C., "A Proposal to Investigate the World Wide Occurrence and Distribution of Thunderstorms by Instrumented Satellites", presented at the 17th International Astronautical Federation Conference, Madrid, Spain, October, 1966.

(59) Massa, R. J. and S. C. Coroniti, "Locating Global Thunderstorm Activity by Satellite", in Vol. 2, p.p. 120 of Ref. 11.

LIST OF TABLES

LIST OF FIGURES